AD-A035 846 DAVID W TAYLOR NAVAL SHIP RESEARCH AND DEVELOPMENT CE--ETC F/G 1/3
THE OVERLAND VERTICAL PLANE DYNAMIC RESPONSE OF THE AALC JEFF (--ETC(U)
JUN 76 D D MORAN

UNCLASSIFIED SPD-615-04 NL

1 OF 1
ADA035846

END

DATE
FILMED
3-77

SPD-615-04

**DAVID W. TAYLOR NAVAL SHIP RESEARCH AND DEVELOPMENT CENTER**

Bethesda, Md. 20084

# THE OVERLAND VERTICAL PLANE DYNAMIC RESPONSE OF THE AALC JEFF(B) ACV; MODEL EXPERIMENTS

by

David D. Moran



APPROVED FOR PUBLIC RELEASE: DISTRIBUTION UNLIMITED

June 1976

SPD-615-04

The Overland Vertical Plane Dynamic Response of the AALC JEFF (B) ACV; Model Experiments

## MAJOR DTNSRDC ORGANIZATIONAL COMPONENTS

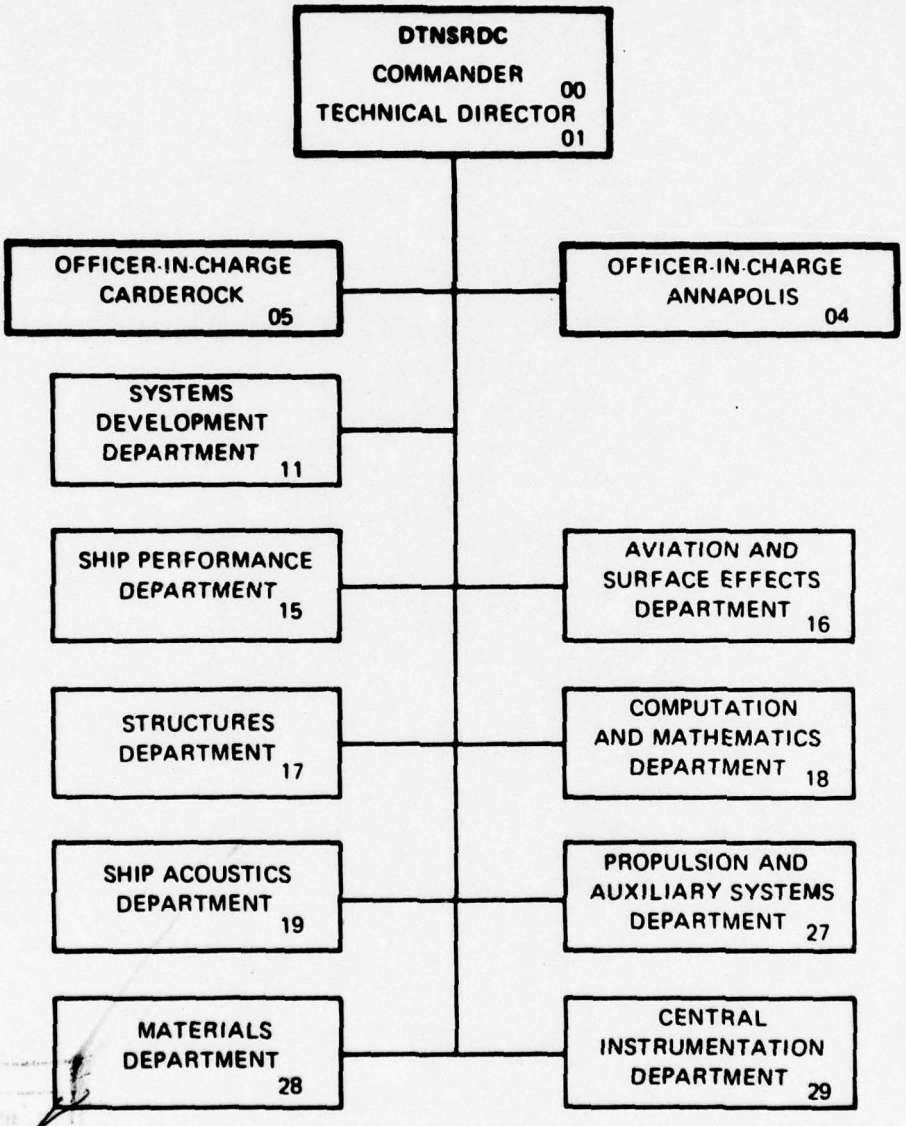

UNCLASSIFIED
SECURITY CLASSIFICATION OF THIS PAGE (When Data Entered)

## REPORT DOCUMENTATION PAGE

READ INSTRUCTIONS BEFORE COMPLETING FORM

(14) 1. REPORT NUMBER: SPD-615-04

2. GOVT ACCESSION NO.

3. RECIPIENT'S CATALOG NUMBER

(6) 4. TITLE (and Subtitle): The Overland Vertical Plane Dynamic Response of the AALC JEFF (B) ACV; Model Experiments

5. TYPE OF REPORT & PERIOD COVERED

6. PERFORMING ORG. REPORT NUMBER

(10) 7. AUTHOR(s): David D. Moran

8. CONTRACT OR GRANT NUMBER(s)

9. PERFORMING ORGANIZATION NAME AND ADDRESS: David W. Taylor Naval Ship Research and Development Center, Ship Performance Department

10. PROGRAM ELEMENT, PROJECT, TASK AREA & WORK UNIT NUMBERS: Work Unit Number 1-1180-004; Task Area S1417

11. CONTROLLING OFFICE NAME AND ADDRESS: Naval Sea Systems Command, Washington, D.C.

(11) 12. REPORT DATE: June 1976

13. NUMBER OF PAGES: 56

14. MONITORING AGENCY NAME & ADDRESS (if different from Controlling Office)

(12) 64p.

15. SECURITY CLASS. (of this report): UNCLASSIFIED

15a. DECLASSIFICATION/DOWNGRADING SCHEDULE

16. DISTRIBUTION STATEMENT (of this Report)

APPROVED FOR PUBLIC RELEASE: DISTRIBUTION UNLIMITED

17. DISTRIBUTION STATEMENT (of the abstract entered in Block 20, if different from Report)

18. SUPPLEMENTARY NOTES

19. KEY WORDS (Continue on reverse side if necessary and identify by block number)

ACV Dynamics, ACV Obstacle Response, AALC JEFF (B) Model Data

20. ABSTRACT (Continue on reverse side if necessary and identify by block number)

The overland dynamic behavior of an air-cushion-supported vehicle is investigated. Experiments have been performed by running the craft over repeated rigid wave forms and allowing it to pitch and heave. Transfer functions relating response variables to the excitation variables are presented. The linearity of the vertical plane dynamics is investigated through a comparison of the response for two different wave heights. Variations in fan speed and fan discharge are also examined. The cobblestone effect, next page

DD FORM 1 JAN 73 1473 EDITION OF 1 NOV 65 IS OBSOLETE
S/N 0102-014-6601

UNCLASSIFIED
SECURITY CLASSIFICATION OF THIS PAGE (When Data Entered)

389 694

cont →created by exciting the craft at a very high frequency, is investigated.

TABLE OF CONTENTS

## LIST OF FIGURES

LIST OF TABLES

## NOTATION

| | |
|---|---|
| $a$ | Wave amplitude |
| $F_n$ | Froude number, $U/\sqrt{Lg}$ |
| $g$ | Gravitational constant |
| $k$ | Wave number, $2\pi/\lambda$ |
| $ka$ | Wave slope |
| $L$ | Cushion length |
| $U$ | Model speed |
| $\lambda$ | Wave length |
| $\lambda/L$ | Nondimensional wave length |
| $\lambda/2a$ | Inverse wave slope |
| $\omega_e$ | Encounter frequency, kU, model scale |

## ABSTRACT

The overland dynamic behavior of an air-cushion-supported vehicle is investigated. Experiments have been performed by running the craft over repeated rigid wave forms and allowing it to pitch and heave. Transfer functions relating response variables to the excitation variables are presented. The linearity of the vertical plane dynamics is investigated through a comparison of the response for two different wave heights. Variations in fan speed and fan discharge are also examined. The cobblestone effect, created by exciting the craft at a very high frequency, is investigated.

## ADMINISTRATIVE INFORMATION

This study was sponsored by the Naval Sea Systems Command under Task Area S1417, Task 14174; and administered by the Amphibious Assault Landing Craft Program Office, Systems Development Department, David W. Taylor Naval Ship Research and Development Center under Work Unit Number 1-1180-004.

## INTRODUCTION

The mission of the Amphibious Assault Landing Craft (AALC) Program Air Cushion Vehicle (ACV) designated JEFF (B) is to transport material from a ship to an off-loading site on a beach. The craft must operate in an overland environment where it is subjected to excitation from the geometrical variations in the ground terrain. The overland dynamic response of the craft may be classified according to terrain or obstacle characteristics. Flat terrain and deformable ground surface variations such as sand, grass, and bushes are not sources of strong excitation, and it is assumed that they will not severely affect the craft. Non-deformable objects on the scale of 10 cm (4 inches) do not excite the craft into oscillation. Examples of these objects are stones and pebbles. A third category includes larger non-deformable objects such as gullies, walls, logs, and large boulders. These are identified as discrete elements large enough to cause the craft to respond but encountered in isolation so that they do not excite it into a steady periodic response. Depending on the size, the obstacle may give rise to large motion which must be modeled nonlinearly, or it may impede the craft completely (the limiting case of nonlinearity). For example, the craft may ride over a wall, be stopped by it, or be deflected at an angle. There are also disturbances which are periodic in nature and which excite a periodic response in the craft. Examples are random terrain over which the craft operates and repeated large obstacles. Other modes of overland operation, such as motion on a slope, can be considered static rather than dynamic and must be analyzed statically.

The overland dynamic behavior of the JEFF(B) was investigated in an experimental program at the David W. Taylor Naval Ship Research and Development Center (DTNSRDC) with several goals in mind. The major goal was to determine all contributions to the dynamic response of the air-cushion vehicle except those associated with the compliant free surface by subjecting the craft to an excitation by periodic waveforms.

This was accomplished by running the craft at a constant speed over a rigid waveform, allowing it to pitch and heave. The result was a set of transfer functions relating response variables to the excitation which consisted of variations of amplitude and wave length. The overland excitation could be of several forms, such as discrete discontinuities in the ground plane, sinusoids, and short, steep waves such as triangular excitations of the type that might be encountered in a real operating environment. A high frequency mode of response encountered in full-scale ACV operation and often referred to as the cobblestone effect was also of interest for experimental investigation. This phenomenon can be examined with very short wave length perturbation fields. Other motivations for investigating ACV overland dynamics included examination of the dynamic effects due to a change in the moment of inertia and examination of the linearity of the response of the vehicle without the complicating aspects of a compliant free surface. Determination of the experimental significance of the internal stability keel in the JEFF(B) design was also of interest. Finally, it was desired to examine the dynamic characteristics of the lift system as manifested in the measurement of discharge of air into the cushion for various excitation frequencies.

In all cases there are several important considerations in studying the response of the craft. If the system is linear, the response to any obstacle can be determined if a transfer function derived from an impulse response or periodic excitation experiment is known. The extent to which transfer functions can be applied is determined by the magnitude of the nonlinearity of the response.

## EXPERIMENTAL INVESTIGATION

### MODEL DESCRIPTION

The air-cushion-supported vehicle chosen for this experimental investigation is a 1/12 scale model of a 150 ton (design displacement) Amphibious Assault Landing Craft. The model, designated as Bell Model B-17, is a dynamic model of the AALC JEFF(B) design. It is a fully-skirted ACV which is designed to operate over water, over solid terrain,

and in surf zones. The basic dimensions and dynamic properties of the JEFF(B) model as tested are listed in Table 1. Detailed plans of the model and a report of early testing of the JEFF(B) model have been published by the Bell Aerospace Company[1*], which was responsible for the design and construction.

## OVERLAND TEST FACILITY AND PROCEDURE

The overland experimental program which is reported in this study was the first to be performed in the United States using a carriage-type facility. The overland rigid-wave experiments were performed on a modified version of the Carriage II facility at DTNSRDC. The 4.05 meter (13.3 foot) wide walkway on the south side of the Carriage II basin was cleared and the rigid-wave field was constructed between the confines of the basin wall and the carriage rail. The JEFF(B) model was then free to move over the artificial terrain on a track parallel to the Carriage II basin. A support structure was mounted to the carriage extending out over this test track. The pitch-heave mechanical system was then attached to the support structure above and fastened to the model below. The carriage was used to tow the model, and the final configuration was very similar to that used in usual seakeeping experiments. Using this towing mechanism the model was free to pitch and heave but was restrained in all other modes of motion. Power to operate the lift fans was supplied from a carriage-borne power source. Data from model-mounted instruments were transmitted through cables to a carriage-borne data processing center.

The rigid terrain consisted of a number of separately tested obstacles of both discrete elements and periodic waveforms. The majority of the data analyzed in this investigation were obtained from periodic excitation by a trapezoidal wave. There are three variables of interest -- craft speed, wave length, and wave amplitude -- and a complete study requires that variations be made in all three parameters. In order to make these variations efficiently, easily, and in a cost-effective manner, it was necessary to use rigid trapezoidal waves with movable ramps and platforms. The trapezoidal waves were constructed of wood and were weighted

---

* Superscripts refer to references given on page 17.

and fixed to the floor to assure an unchanging terrain. The ground over which the experiments were performed was reasonably flat, but variations of approximately 2.5 cm (1 inch) could be found. Adjustments had to be made to obtain a zero mean level for the trapezoid. The trapezoidal configuration allowed a complete spectrum of excitation (encounter) frequencies to be examined through systematic changes in wave length and carriage speed. Sinusoidal excitation was prohibited by the cost and difficulty of making systematic variations in wave length. The cobblestone-effect response which is described in detail in the following section, was excited by placing construction-grade wooden 2x4's at equal spacings, producing a square wave with the dimensions of a commercial 2x4. The geometrical details are given along with other operational conditions in Table 2.

A trapezoidal waveform produces an excitation which is high in harmonic content above the fundamental. Preliminary analysis and experimentation demonstrated that the multiple harmonic excitation was not detrimental to the experiments performed. In general it should be noted that the third, fifth, and higher harmonic components of the excitation by a trapezoidal waveform were in effect no larger than those encountered in a regular-wave seakeeping experiment in which the waves are produced by a pneumatic wavemaker. (All even-numbered higher harmonic components of a trapezoidal waveform are identically zero.) Coefficients of the trapezoids employed in this experimental investigation are given in Table 3.

There are certain advantages to be gained from an overland investigation. Experiments can be exactly repeated because of the rigid waveforms employed. The linearity of the craft response can be examined easily because the excitation is precisely known. Fine control can be exercised over the geometric form of the excitation. The trim of the craft can be fixed with a greater degree of accuracy overland than in over water operation. Among the disadvantages is the obvious lack of free surface deformation. Overland experiments are more expensive and more difficult than over water programs because each waveform must be

constructed individually, and they lack the rapid flexibility for changing waves found with over water experiments. Much of the instrumentation and the support structure must be especially constructed since overland testing is presently an uncommon test procedure.

## INSTRUMENTATION

The craft instrumentation consisted of pitch and heave transducers, seven pressure transducers, two vertical accelerometers, and an ultrasonic wave height transducer. A hot-wire anemometer measured the discharge through the forward lift fans. The locations of the instrumentation relative to the center of gravity of the model are indicated in Table 4.

An ultrasonic wave-height sensor employed in the experiment was attached to the carriage and located alongside the model adjacent to the model center of gravity. The recorded elevations of the terrain measured as the carriage and model passed over the rigid waveforms were used in the harmonic analysis described in the following section.

Vertically-oriented accelerometers were located at the center of gravity of the model and at a point near the bow. The heaving and pitching motions of the craft were determined through linear potentiometers attached to the heave staff (or tow pivot).

Prior to the initiation of the overland experimental program the JEFF(B) model was carefully tuned to operate at the correct cushion pressure and bag pressures for the appropriately scaled values of displacement and moment of inertia. The pitch moment of inertia and the vertical position of the center of gravity were adjusted to correspond with experimental values recorded in previous experiments. The model was then operated on-cushion in a lightly-tethered condition and allowed to assume equilibrium trim conditions. The cushion pressure in each cell of the segmented cushion was measured and the bag pressures were monitored as the air vent holes between the bags and fingers were closed or opened individually to determine the effect of lift system discharge on the bag and cushion pressure distributions. The model was therefore trimmed to equilibrium conditions with a cushion pressure uniform to within 2 percent. The overpressure in the bow bag was stabilized at a value of

1.31 and the final stern bag overpressure ratio was 1.53. The side bag overpressure ratio remained a function of position but was equal to approximately 1.4.

## DATA COLLECTION AND ANALYSIS

Time histories of the output of the pressure transducers, accelerometers and ultrasonic wave height transducer were digitized and stored on magnetic tape through an Interdata computer. Following a successful run over the fixed terrain the digitized data were harmonically analyzed to compute the first, second, third and fifth harmonic amplitudes and phases. The product of any particular run was therefore a listing of the harmonic characteristics (amplitude and phase) of the recorded signals. The phase angle in each case was referred to a defined zero for a wave peak at the model center of gravity. The model speed and known wave length were input variables to the harmonic analysis so that an integer number of encountered waves was analyzed. The particular number of waves analyzed was a function of (and less than) the number of wave cycles available, but in each case the first complete excitation cycle was excluded from the analysis to allow the model to stabilize into an equilibrium mode of motion. Although there is no analytic benefit resulting from the analysis of more than one regular cycle of any variable, experience with the system indicated that the numerical accuracy of the procedure was improved through an analysis of several cycles. This process is equivalent to the arithmetic average of the harmonic analysis of a number of individual cycles.

## PREVIOUS EXPERIMENTAL RESULTS

In a preliminary experiment preceding this study the cushion pressure and acceleration response of the AALC JEFF(B) air-cushion-supported vehicle to a number of solid obstacles and solid terrain configurations were examined. The results of these initial experiments have been reported by Moran, Pemberton, and Knight.[2] Through these experiments it is found that the model scale step height limitation is approximately 5 cm (2 inches) for forward operation of the craft. For heights above this limitation the bow bag of the model cushion bow seal catches at the point where the bow fingers attach, deflates, and folds

under the model until the hard structure at the bow contacts the surface of the step. If the step has a leading edge ramp with an angle no greater than the angle of the bow fingers, the model can pass freely over the obstacle at any speed. In the reverse direction the model can pass freely over a step which has a leading edge ramp with a 45 degree slope. However, it is found that the model will not back over step discontinuities at ground level at any speed unless the step height is extremely small.

In the same experimental program the heave natural frequency is found to be approximately twice that for pitching or rolling motion. The model experiences large variations in bow acceleration and cushion pressure as it passes over terrain elements of steps, pulses, and pulse trains. The most dramatic variations occur when the bow seal vents to the atmosphere as the model encounters a step down in surface elevation. Vertical motion shows no indication of instability, but an apparent yaw instability is detected for terrain encounters with an initial yaw angle and an initial nonzero yaw rate.

An extensive analysis of the cushion pressure distribution and the acceleration response of the JEFF(B) has been performed by Moran and Schechter,[3] based on results obtained from the same experimental program from which the present study's data is derived. They report on all measured model accelerations, and those results are not duplicated here. A complete analysis of cushion pressure measurements was made in which these data were analyzed to determine the significance of the spatial pressure distribution. It is shown that the spatial pressure distribution is the major mechanism for pitch excitation but that heave motion is more dependent upon other mechanisms, probably deformations of the bow and stern seals. The effect of the internal stability keel on the vertical plane response is investigated by a comparison of experiments repeated for identical operating conditions with and without the stability keel in place. It is found that the heave dynamics are not affected but that the pitch dynamics are degraded by removal of the stability keel. Heave response is severely affected by small changes in the longitudinal position of the stability keel.

Moran[4] has presented an analytical model of the overland dynamics of the JEFF(B) air-cushion-supported vehicle in two degrees of freedom. The data included in the present study are used extensively in the report on the dynamic model to provide simulation verification for the analytic model.

## EXPERIMENTAL RESULTS

The complete overland frequency response characteristics of the AALC JEFF(B) model obtained through the experimental program are summarized for the pitch and heave response in Figures 1 and 2. The pitch transfer function is defined as the first harmonic amplitude of the pitch response normalized by the wave slope, ka. Similarly, the heave transfer function is the first harmonic amplitude of the heave response normalized by the wave amplitude, a. The results are presented for constant speed U as a function of nondimensional wave length $\lambda/L$. The experiments were conducted by holding the wave length constant and varying the speed over a range of 2 to 7.7 m/sec (4 to 15 knots) model scale, corresponding to a Froude number ($F_n$) range of .46 to 1.74. The equivalent full-scale JEFF(B) speeds lie between 7 and 26.7 m/sec (13.9 and 52 knots). The pitch transfer functions are presented as a best fit to the complete experimental data set shown in Figure 3 and the heave transfer functions to the experimental data shown in Figure 4.

There is experimental verification of a null point in the region of unity ($\lambda/L=1$) for heave, but the data summaries of Figures 1 and 2 have been prepared to illustrate the behavior only for values of wave length greater than unity ($\lambda/L>1$). Even though some data were collected for wave length ratios less than unity ($\lambda/L<1$), they provided insufficient evidence from which to construct performance curves based solely on experimental data for small wave lengths. Null response at unity wave length for heave can be seen for each tested speed, and this behavior appears to be independent of speed for speeds less than 4m/sec (8 knots). A complete reporting of the heave transfer function in the wave length domain would include behavior below the unity wave length. It is expected that null response would be evident at wave length ratios of 1/2, 1/3, 1/4, .... . For long wave

lengths ($\lambda/L>5$), the asymptotic response of the craft is represented by unity values of the pitch and heave transfer functions. This behavior is evident for both response variables in the presentation of the reported experimental data, but the pitch response shows a more rapid attainment of the asymptotic level than that observed for heave.

The pitch response seen in Figure 1 has a generally stronger peaking character with increasing speed. The resonant condition, with a magnitude greater than 1.6, occurs at a wave length ratio of 2 ($\lambda/L=2$) for the highest speed tested (U=7.7 m/sec, $F_n=1.74$). For wave length ratios greater than 2, there is generally a higher pitch response with increasing speed; but for wave length ratios less than 2 the response magnitude may be inversely proportional to speed. There is an uncertainty concerning possible null point behavior at half cushion lengths ($\lambda/L=0.5$) for pitch. There appears to be a tendency for the null point to occur at longer wave lengths with increasing speed. The evidence is not conclusive because experimental data is insufficient in the range of wave lengths less than 1.3.

In comparison with pitch, the heave response in Figure 2 is subject to more cushion dynamic damping, with the damping appearing to decrease with increasing speed. As in the case of pitch, it appears that the heave response increases with speed for wave length ratios greater than 2, except for the experimental results provided at a speed of 6 m/sec (12 knots, $F_n=1.39$) which show a high value of heave magnification for a wave length ratio of 5 ($\lambda/L=5$). This should not be accepted as a general result, however, since the long-wave-length end of the curve is determined by a single data point. An interesting feature of the heave transfer function for this speed is the change in slope for a wave length ratio of 1.75 ($\lambda/L=1.75$). Again, although there is not the amount of evidence that one would wish to see to verify this behavior, there was a strong attempt to make the summary curves as truly representative of the actual data as possible.

The curves in Figures 1 and 2 are derived from a best fit to the heave and pitch data sets which are shown in Figure 3 for pitch and Figure 4 for heave. In both of the latter figures, data are included

for two wave lengths with wave length ratios less than unity; however, no graphical interpretation is attempted for these isolated points because of an insufficient number of wave lengths examined. Overland experiments are more difficult than seakeeping experiments because each wave must be constructed separately, and it is therefore time-consuming and expensive to construct full, well-documented transfer functions.

The same transfer functions for pitch and heave are presented in Figures 5 and 6 as a function of encounter frequency $\omega_e$ for fixed values of wave length $\lambda/L$. This method of presentation shows the behavior of the craft over land in a manner equivalent to that employed to show transfer functions for the over water case and thus provides a comparison between the two cases. Consideration of the response as a function of encounter frequency also shows the resonant frequencies for overland operation.

The pitch transfer function is shown for decreasing values of wave length $\lambda/L$ in Figures 5a through 5g. As the wave length decreases the magnitude of the zero frequency asymptote of the curve begins to decrease. It is not possible to demonstrate the asymptotic value experimentally with the present data for small wave lengths. However, when response data are presented in the frequency domain for fixed wave lengths there is reason to expect that the pitch transfer function will not approach unity at zero frequency for overland operation as the wave length becomes very small. See for example Figure 5f, with a wave length ratio of 1.32. When the craft is on a slope, moving either up or down, the craft length extends far over the length of the slope onto the crest and trough. The equilibrium pitch angle is always smaller than the slope of the rigid wave, and therefore the transfer function approaches zero at zero speed corresponding to zero frequency for a fixed wave length.

The resonant behavior of the JEFF(B) overland is clearly indicated in Figures 5d, 5e, and 5f at a frequency of approximately 12.5 radians/second. The resonant frequency appears to increase slightly with decreasing wave length as the wave length varies from 1.67 to 1.32,

and the transfer function magnitude decreases with decreasing wave length, varying from 1.35 at a wave length of 1.67 to 1.0 at a wave length of 1.32. Figure 5c shows incipient resonance, but no data were collected for supercritical conditions over this wave length. For very large values of encounter frequency, the pitch transfer function exhibits the expected rapid decay with increasing frequency, as demonstrated in Figures 5e and 5f. Finally, the pitch transfer function for a wave length of .91 is shown in Figure 5g. It should correspond to null-type behavior, and, indeed, the variation is small and fairly uniform over the frequency range tested.

In a manner similar to that previously discussed for pitch, the heave transfer function does not approach unity for zero frequency when the response function is presented for fixed wave length operating conditions. As with pitch, there is a physically justifiable reason for the observed asymptotic behavior. For static conditions (zero speed and zero frequency), when the craft is on a crest there is a tendency for the skirts to contour the crest and therefore the flying height is lower with respect to the peak of the rigid wave at the crest than that observed on level ground. Similarly, for static conditions in a wave trough the craft is supported by the bow and stern seals and the flying height is higher with respect to the trough elevation than that which would be measured over level ground. Thus the heave response static value is expected to be less than the wave amplitude, and for zero frequency the heave transfer function is justifiably less than unity. This condition becomes increasingly evident as the wave length is shortened.

The resonant condition for heave is demonstrated in Figures 6d, 6e, and 6f. In a manner similar to that seen for pitch, the resonant frequency varies from 13 to 14 radians/second, depends on wave length and increases with decreasing wave length. Further, the magnitude of the heave transfer function at the resonant point is seen to decrease with decreasing wave length, as was seen in the case of pitch. An approximate null point is demonstrated for heave in Figure 6g for a wave length of .91.

The pitch and heave transfer functions were shown previously as functions of wave length for fixed speed in Figures 1 and 2. To provide a further clarification of the overland response, the pitch and heave transfer functions are presented in the wave length domain for fixed encounter frequency in Figures 7 and 8. Since the data is a cross-plot, there is significant scatter in the data points which define the constant frequency response. However, several points are evident from these results. It can be concluded for both pitch and heave that for any fixed wave length the vertical plane dynamic response increases with encounter frequency; or, alternately, for any fixed encounter frequency, the response increases with wave length for all wave lengths greater than unity over the range of wave lengths tested. It should be expected that the response curves for high frequencies will decline for increasing wave length, but insufficient data were collected to demonstrate this phenomenon clearly.

As a further part of this study a small amount of data was collected to begin to provide a demonstration of the linearity of the response of the craft. Data are provided in Figures 9 and 10 for pitch and heave response in the frequency domain for nearly identical wave lengths. In general, the pitch and heave response was tested at two values of inverse wave slope, $\lambda/2a$, equal to 34 and 56 respectively. Although these values are not sufficiently different to demonstrate conclusively the extent of nonlinearity in the response of the air-cushion-supported vehicle, it appears that both pitch and heave responses are slightly less for steeper waves. For pitch, this conclusion appears to be most evident for frequencies less than the resonant frequency. However, the opposite is true for heave, and slightly nonlinear behavior is more pronounced for frequencies greater than the resonant frequency. A complete examination of linearity in the response of an ACV obviously requires more experimental evaluation over a broader range of wave heights and should be examined over a range of wave lengths as well.

As part of the overall characteristics of the craft, it is of interest to examine the effect of fan speed as a lift system characteristic

parameter on the pitch and heave overland dynamics of the craft. As shown in Figure 11, small variations (6 percent decrease and 30 percent increase over the normal operating level) in fan speed produce negligible changes in the pitch response. However, as should be expected, changes in fan rotational speed do affect the heave response seen in Figure 12, with an indication of increasing heave stiffness with increasing fan speed. Although fan discharge curves are not included, increasing fan speed corresponds to increasing fan discharge at an approximately constant fan discharge pressure.

During the course of the experiments, the pitch moment of inertia was decreased by 4 percent. The effects of this small change are shown in Figures 13 and 14; unfortunately, the change was not significant enough to afford an opportunity to draw conclusions regarding the effect of inertia on the pitch-heave dynamics.

Throughout the development of operational hovercraft, there have been indications of a high frequency response which has often been described as the cobblestone effect. To examine this phenomenon experimentally on a model scale, two specific waveforms were constructed to generate a high frequency excitation. The first consisted of rigid triangular waves with a wave length $\lambda/L$ of .46 and an inverse wave slope $\lambda/2a$ of 33. The craft was tested over this waveform with increasing speed at frequencies ranging between 15 and 55 radians/second. As shown in Figures 15 and 16, the pitch response is almost zero over the entire frequency range, and the heave response is low but increasing slowly with increasing frequency. To extend further the tested frequency range, a square wave was constructed with a nondimensional wave length $\lambda/L$ of .09 and an inverse wave slope $\lambda/2a$ of 3.9, allowing the determination of craft response over a frequency range between 3 and 95 radians/second. An indication of a rather high pitch response at a frequency of 5 radians/second and a secondary peak at the previously determined resonant frequency of 13 radian/second can be seen in Figure 17. More importantly, the pitch response of the craft appears to reach a peak for an encounter frequency greater than 75 radians/second. A slightly different response is shown for heave, for which the resonant

frequency occurs at 13 radians/second. The heave response appears generally to increase with increasing frequency. Interestingly, in the frequency range between 25 and 55 radians/second, the pitch and heave response functions measured for the square wave excitation correspond fairly closely to the response observed over the triangular wave as presented in Figures 15 and 16. As a final indication of the apparent cobblestone effect observed on a model scale, the acceleration of the center of gravity and the bow acceleration are indicated in Figure 18. The acceleration levels generally increase with encounter frequency, and the bow acceleration appears to approach a maximum value at a very high encounter frequency (greater than 90 radians/second).

Finally, in order to measure the discharge of the lift system at the exit of the port fan, a hot-wire anemometer was placed at the center of the exit stream in a flow region which was found to be approximately uniform. The probe could be monitored to indicate the continually changing velocity in the duct. As the craft was excited periodically, the discharge in the lift system changed in a periodic manner. The varying flow velocity was analyzed harmonically and found to contain manifold higher harmonics, making interpretation of the higher harmonic content difficult. The total energy in the disturbed discharge was computed and is presented as the nondimensionalized standard deviation of fan discharge as a function of encounter frequency in Figure 19. The craft was run at forward speed over flat terrain, and, due to turbulence and other effects, the flow was found to contain unsteady energy at zero excitation frequency as measured by the monitored fan discharge. This zero-frequency discharge was used to nondimensionalize the data presented in Figure 19. The response has been displayed for approximately constant values of wave length in the encounter frequency domain. Although there is significant scatter in the data, there is a definite trend toward increasing amplitude of fan flow response with increasing encounter frequency. It is to be expected that the fan flow variations would decrease at some very high frequency, but no experimental evidence of this behavior was detected.

## SUMMARY

Experimental investigation of the overland behavior of an air-cushion-supported vehicle has increased the available information concerning the dynamic response of this craft to passage over rigid surfaces. In a number of the experiments the craft was run at varying speeds over rigid trapezoidal waves for which the wave length was held at several constant values. Experimental verification of null point behavior for a wave length equal to the cushion length is seen in the heave response, but more experimental data for shorter wave lengths are necessary for a complete demonstration of null response in both heave and pitch. There is, however, an indication that the heave null point moves to increasing wave length values with increasing speed, implying that the "dynamically-effective" cushion length is a decreasing function of speed even though the actual length remains fixed. In order to demonstrate this null point behavior, additional experimentation would have to be performed in the range of normalized wave lengths between 1 and 1.3.

The pitch and heave response is in general dependent on the wave length and speed; however, for Froude numbers less than unity the response tends to be independent of speed. Resonant conditions are clearly evident in the experimental data, with the pitch peak response occurring at approximately 12.5 radians/second and the peak response in heave between 13 and 14 radians/second.

Experiments were performed for two values of wave slope over a fixed wave length. The response shows generally linear behavior, but the wave slopes were not sufficiently different to demonstrate linearity conclusively from the present data. Increasing the fan speed causes an increase in the heave transfer function but does not affect the pitch of the craft. When the craft is run over square waves, it is possible to see a pitch-heave resonant frequency at 13 radians/second, a sub-resonant frequency at 5 radians/second for pitch, and an appearance of the cobble-stone effect in the range between 75 and 95 radians/second. Finally, in an examination of variations in fan discharge, the amplitude of the oscillations of velocity in the lift system increases with wave length and with encounter frequency.

## REFERENCES


1. Bell Aerospace Company, "Preliminary Design Summary Report-AALC C 150-50", Bell Aerospace Company Report No. 7385-950007 (Oct. 1970).
2. Moran, David D., T. Michael Pemberton, and Kenneth S. Knight, "A Preliminary Experimental Investigation of the Overland Behavior of the JEFF(B) Amphibious Assault Landing Craft", NSRDC Ship Performance Department Report No. SPD-615-01 (Mar. 1975).
3. Moran, David D. and Richard S. Schechter, "The Vertical Motion of an Air Cushion Vehicle and the Spatial Distribution of Cushion Pressure", DTNSRDC Ship Performance Department Report No. SPD-615-02 (Apr. 1976).
4. Moran, David D., "A Nonlinear Vertical-Plane Mathematical Model for Air-Cushion-Supported Vehicles", DTNSRDC Ship Performance Department Report Number SPD-615-05 (June 1976).

## ACKNOWLEDGMENTS

The author would like to express his appreciation to those people who aided in the design and execution of the experimental program which furnished the data presented in this study. James A. Kallio and T. Michael Pemberton were responsible for the preparation of the experiments, and Kenneth S. Knight performed preliminary experimental work. William B. Dixon, Daniel Huminik, and Gordon R. Minard developed and monitored the instrumentation used for the experimental program. Hugh Y. H. Yeh, Richard F. Messalle, Richard S. Schechter, and Allen H. Magnuson are thanked for their performance during the test program and Michael J. Davis and J. Brooks Peters for the development of data analysis routines.

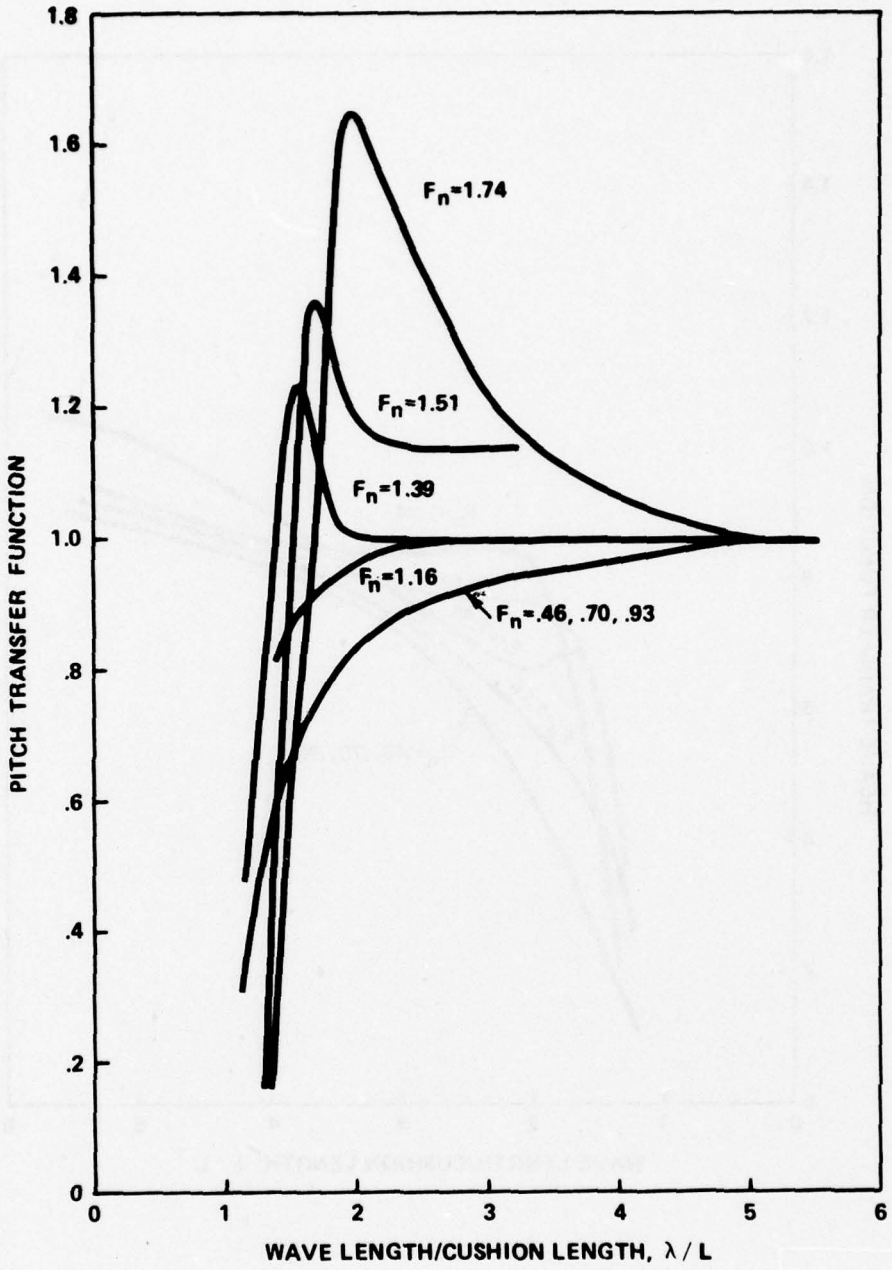


Figure 1 - Pitch Transfer Function as a Function of Wave Length for Constant Froude Number

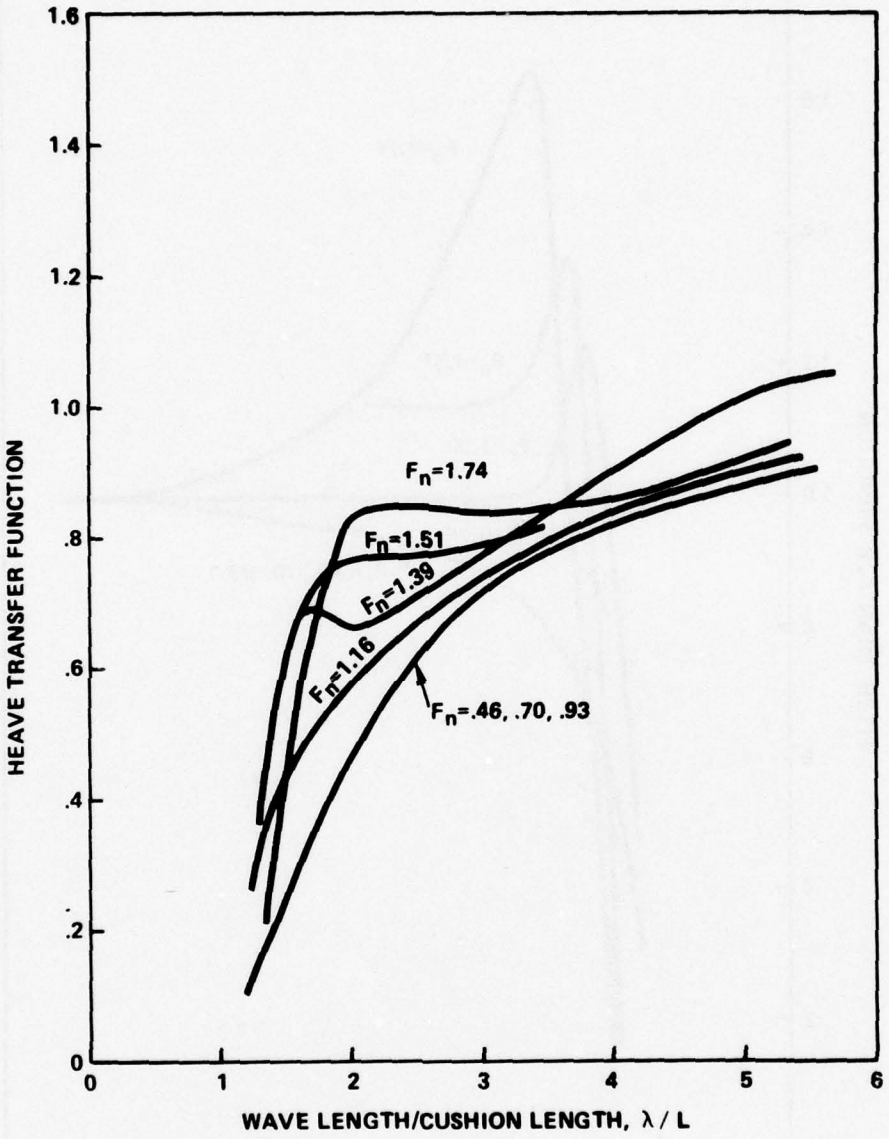


Figure 2 - Heave Transfer Function as a Function of Wave Length for Constant Froude Number

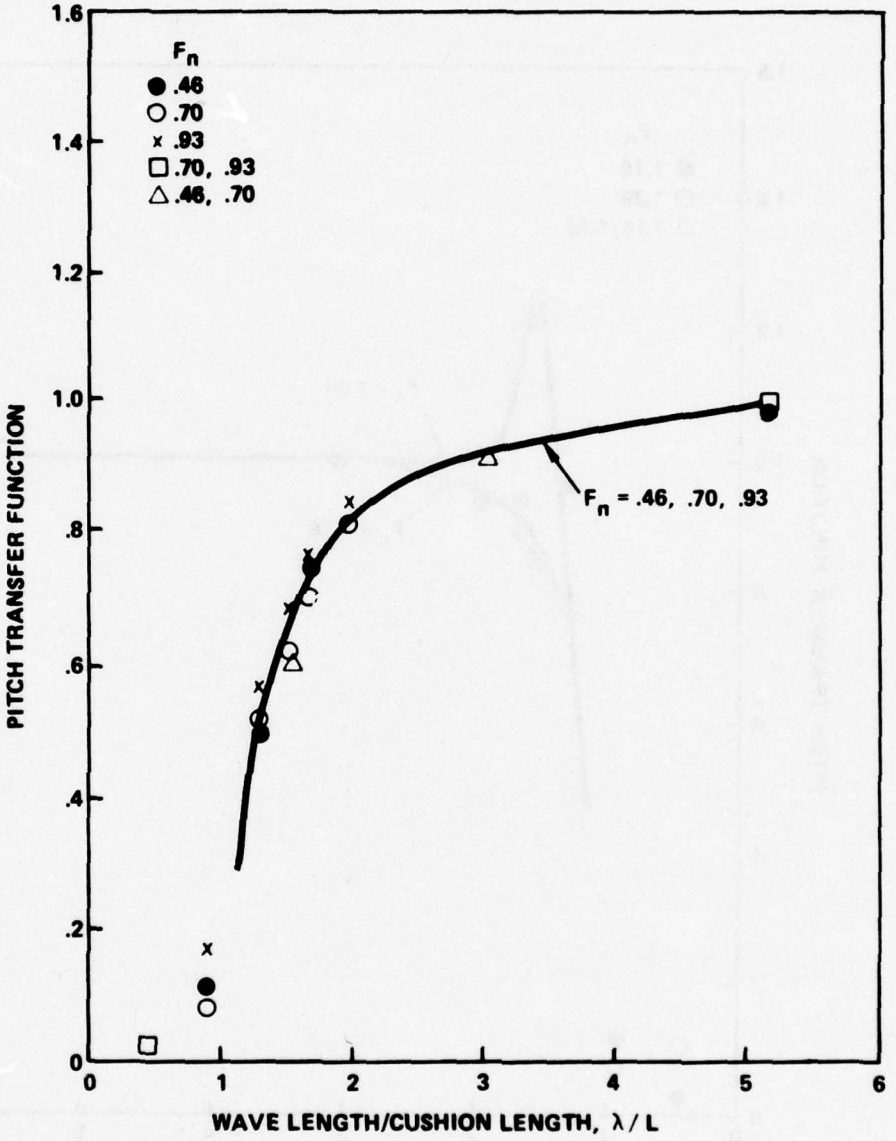


Figure 3a - Pitch Transfer Function as a Function of Wave Length for $F_n$ = .46, .70, .93

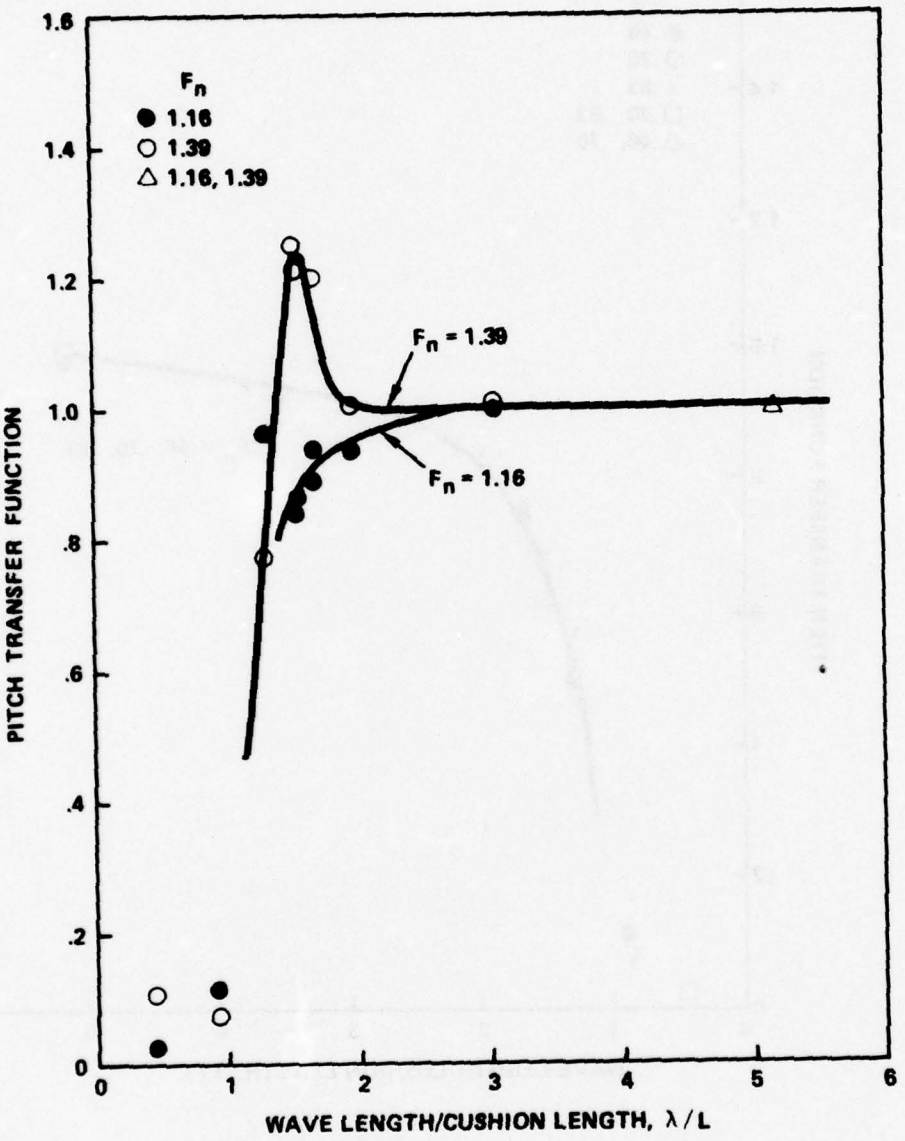


Figure 3b - Pitch Transfer Function as a Function of Wave Length for $F_n$ = 1.16, 1.39

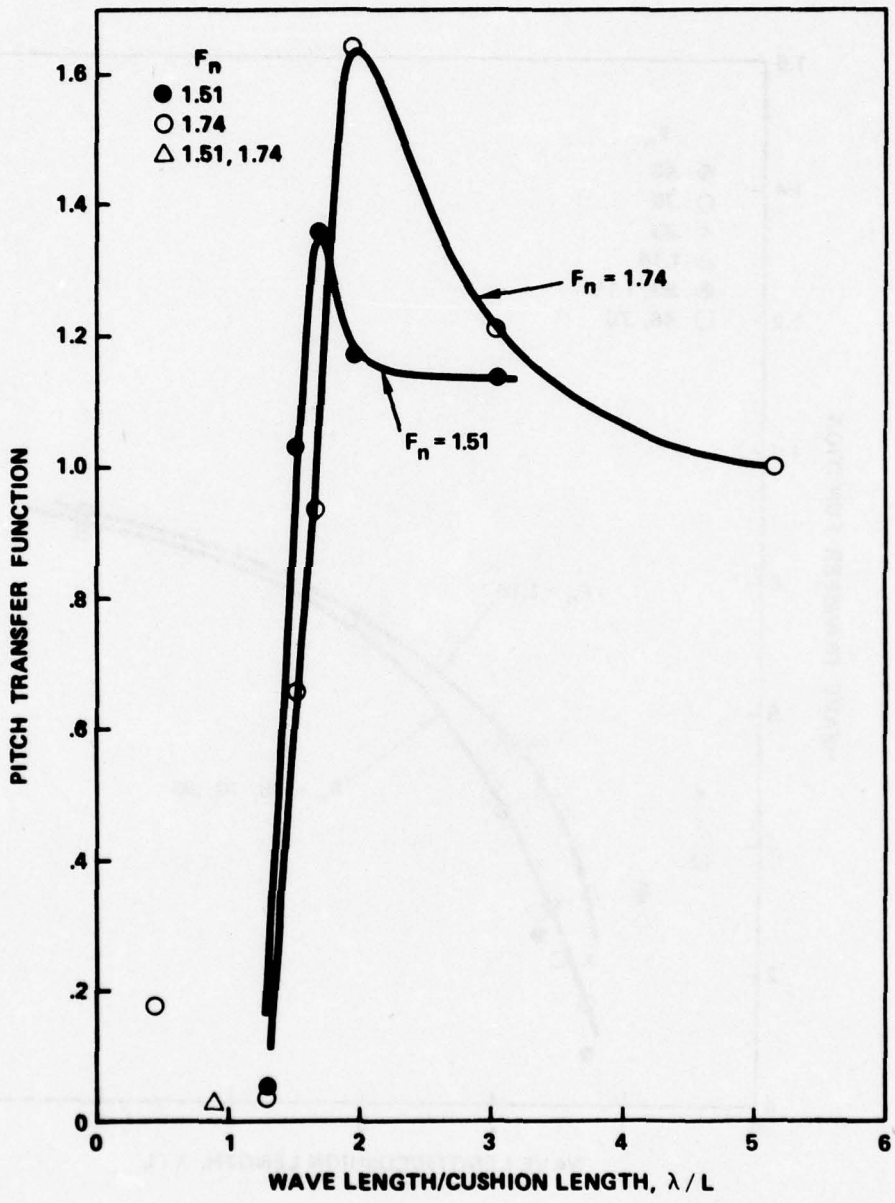


Figure 3c - Pitch Transfer Function as a Function of Wave Length for $F_n$ = 1.51, 1.74

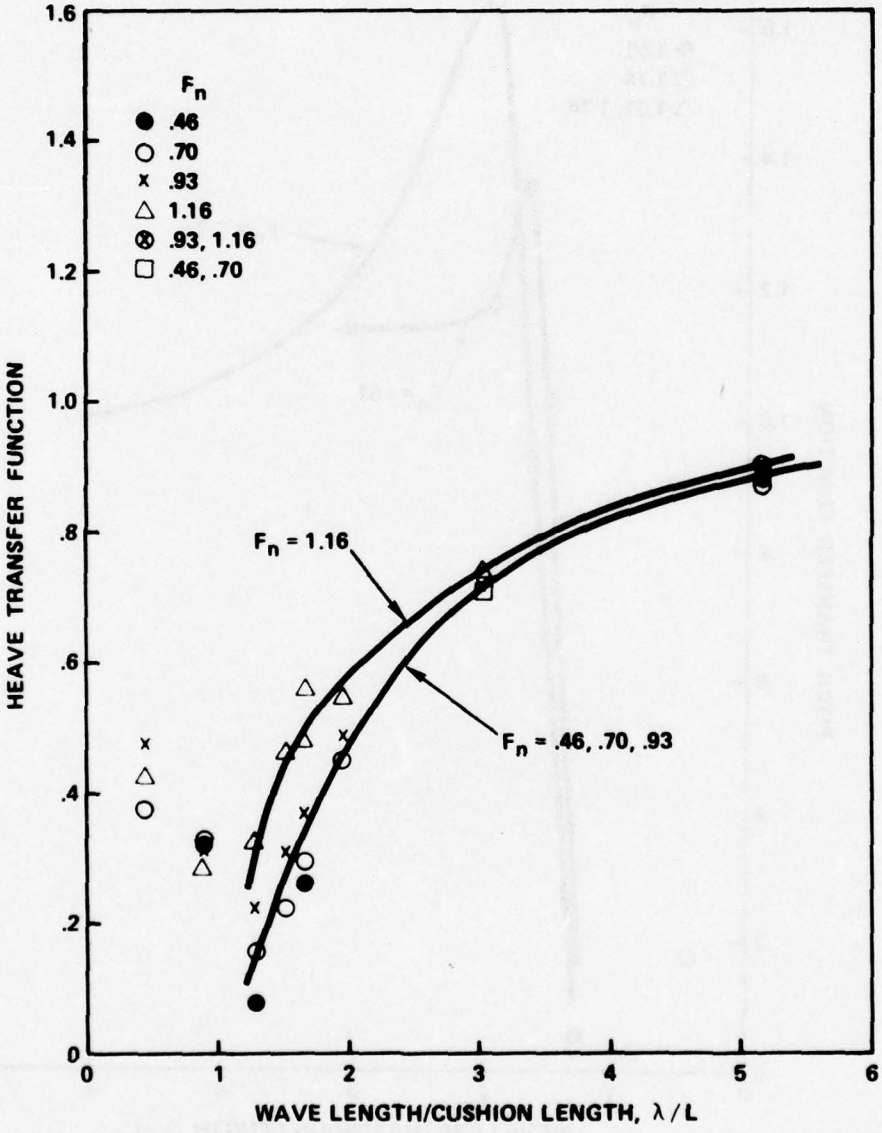


Figure 4a - Heave Transfer Function as a Function of Wave Length for $F_n$ = .46, .70, .93, 1.16

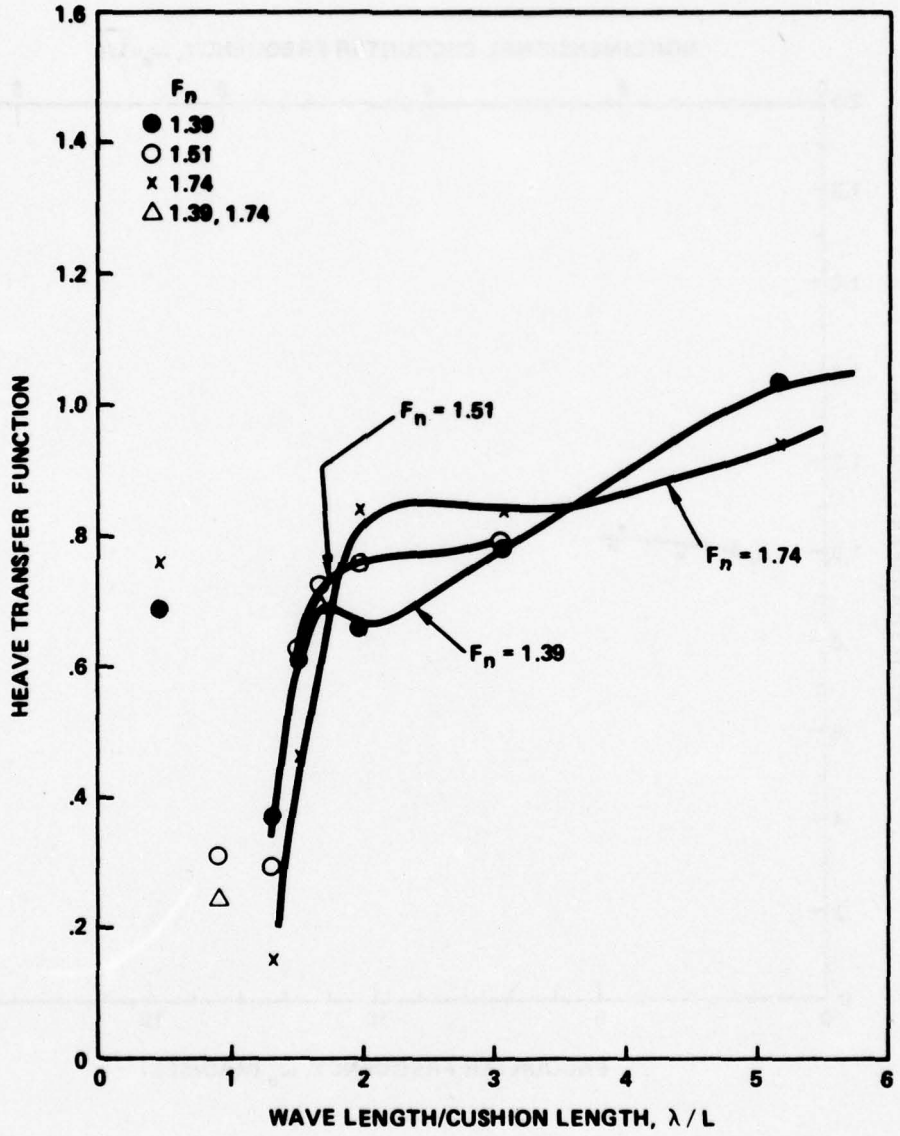


Figure 4b - Heave Transfer Function as a Function of Wave Length for $F_n$ = 1.39, 1.51, 1.74

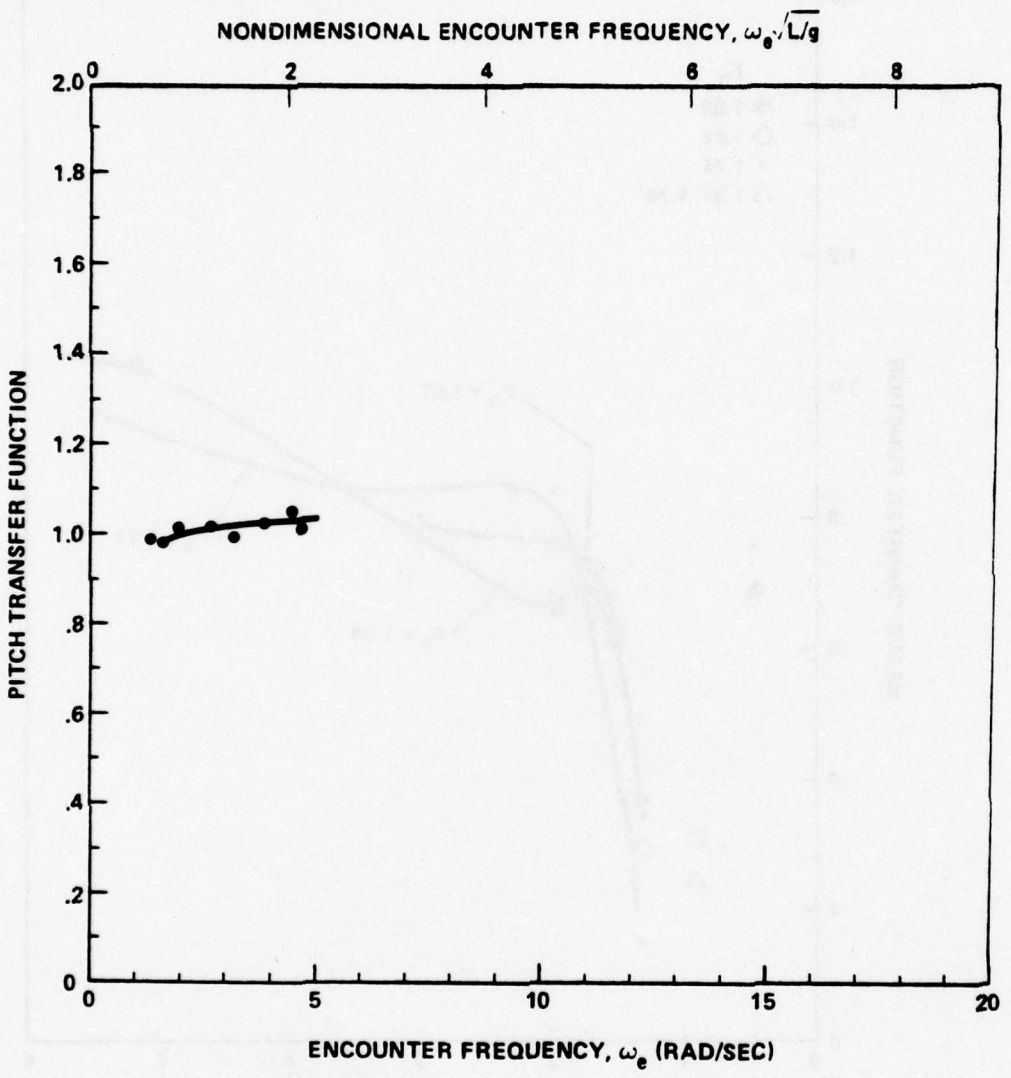


Figure 5a - Pitch Transfer Function as a Function of Encounter Frequency for $\lambda/L = 5.17$

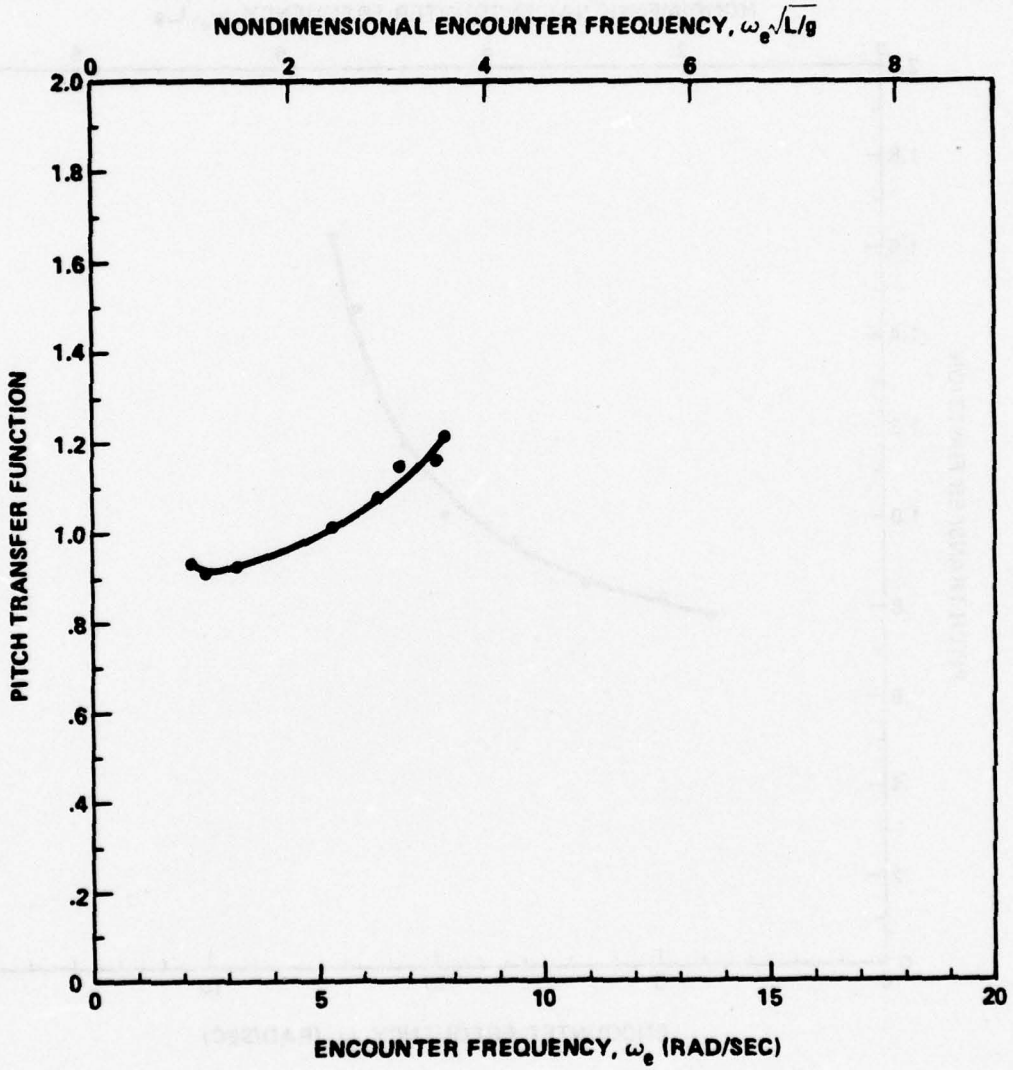


Figure 5b - Pitch Transfer Function as a Function of Encounter Frequency for $\lambda/L = 3.04$

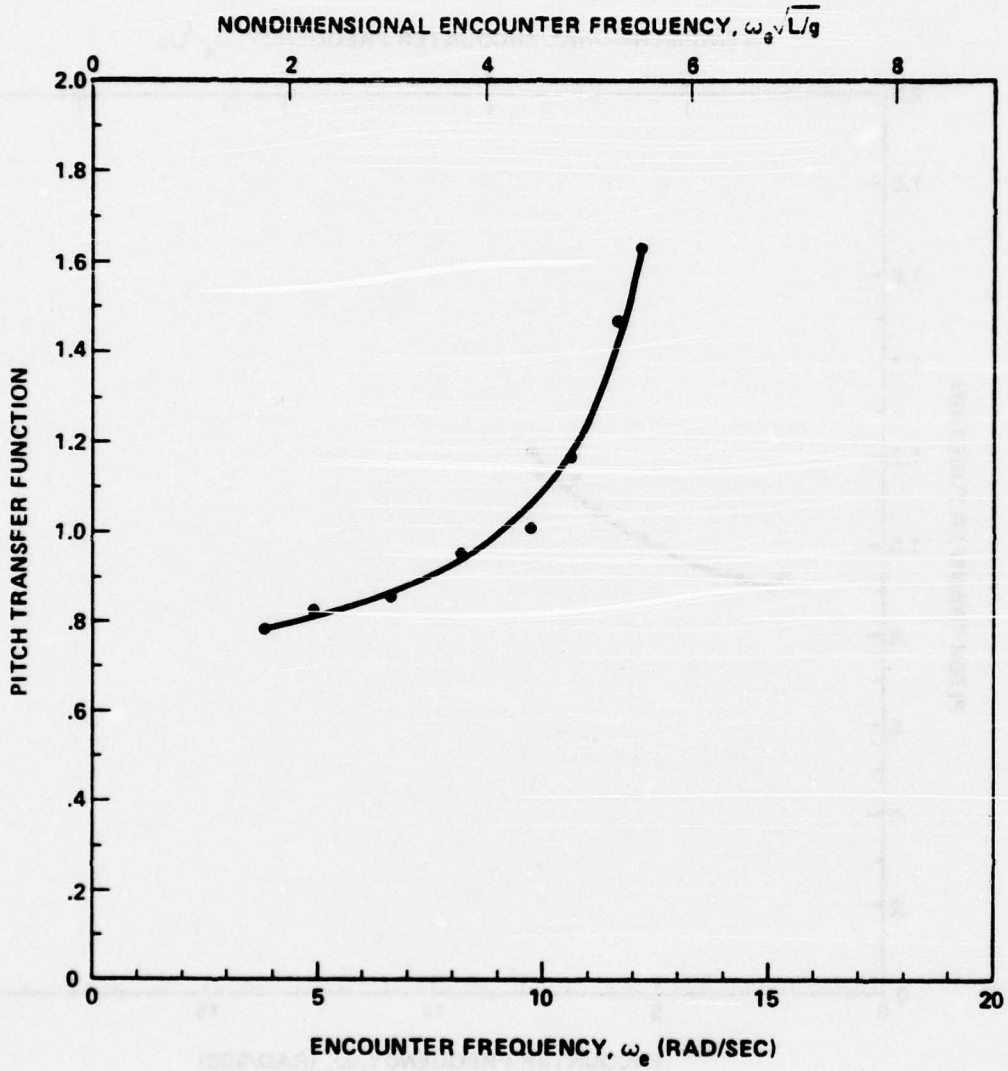


Figure 5c - Pitch Transfer Function as a Function of Encounter Frequency for $\lambda/L = 1.98$

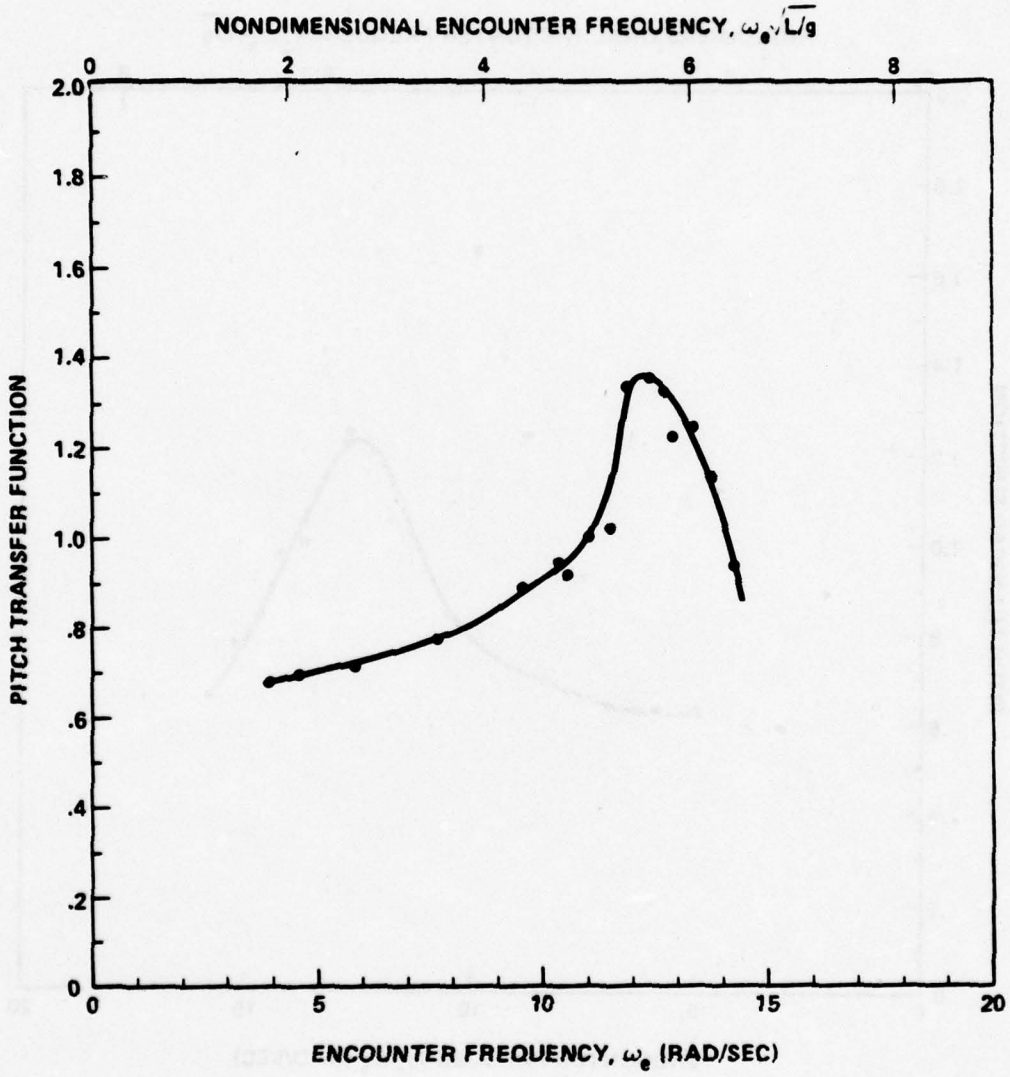


Figure 5d - Pitch Transfer Function as a Function of Encounter Frequency for $\lambda/L = 1.67$

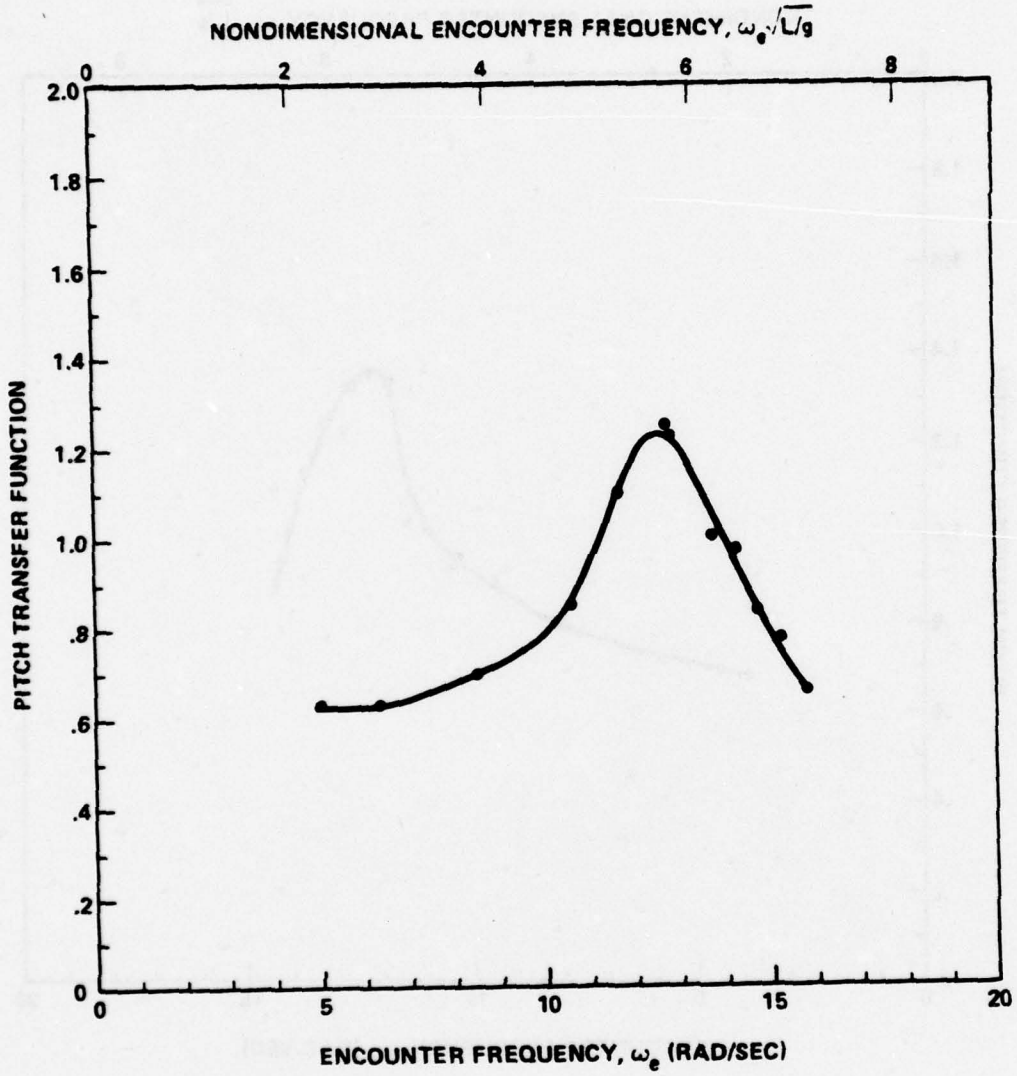


Figure 5e - Pitch Transfer Function as a Function of Encounter Frequency for $\lambda/L = 1.52$

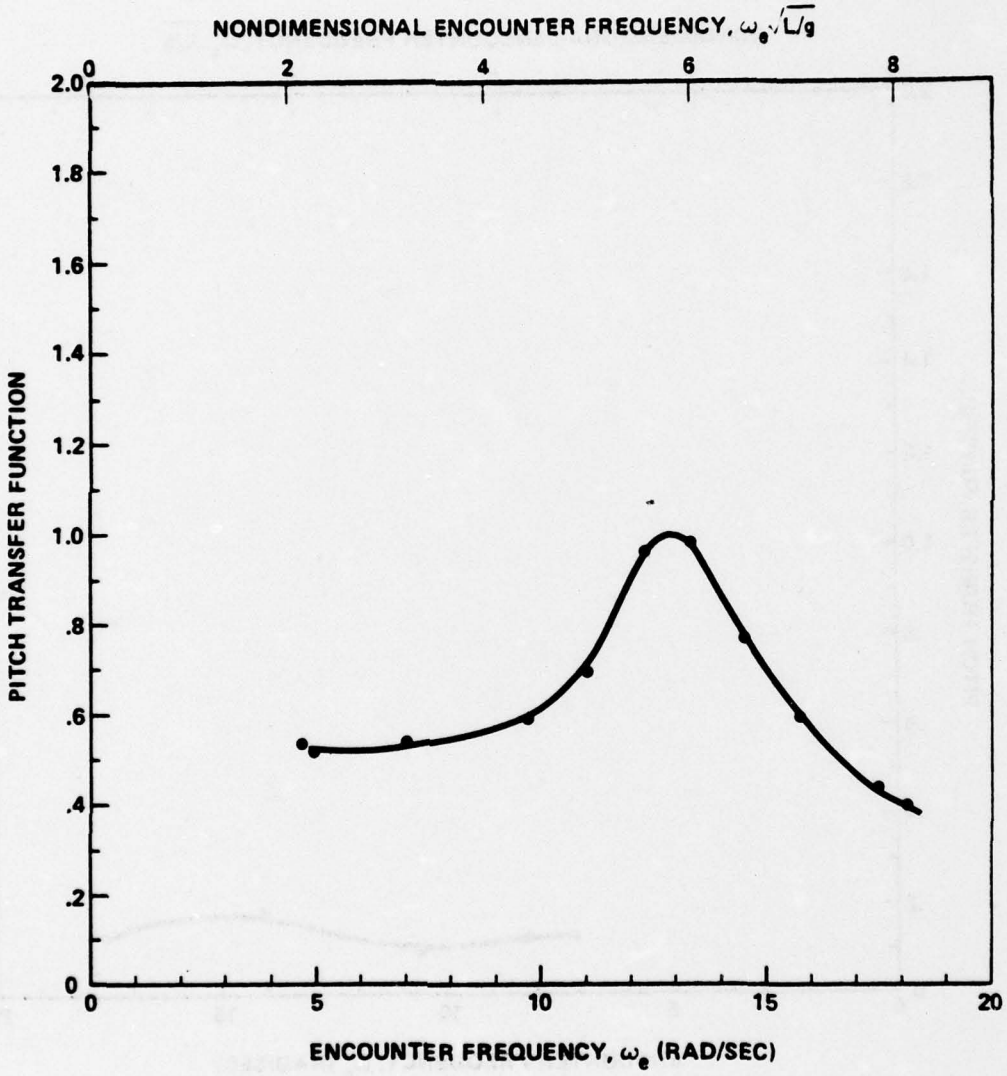


Figure 5f - Pitch Transfer Function as a Function of Encounter Frequency for $\lambda/L = 1.32$

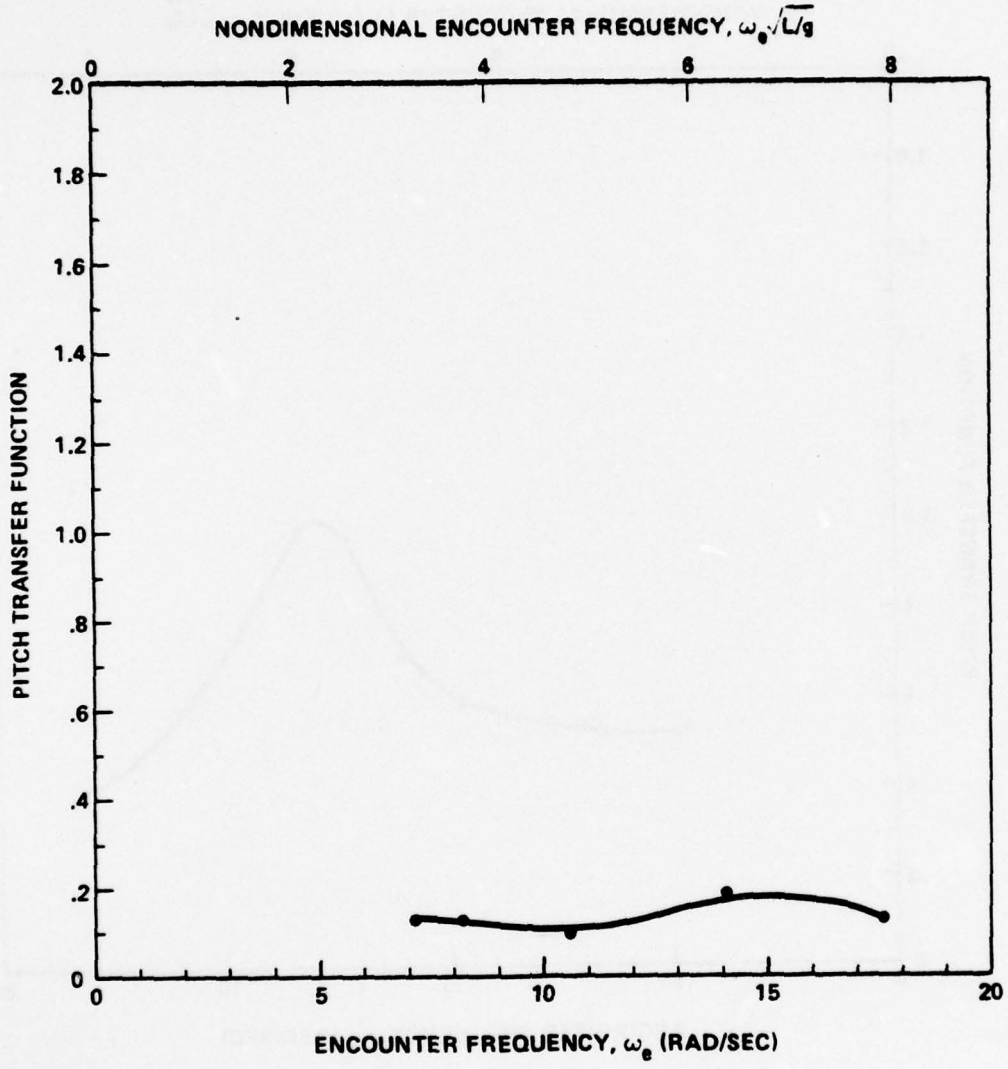


Figure 5g - Pitch Transfer Function as a Function of Encounter Frequency for $\lambda/L = .91$

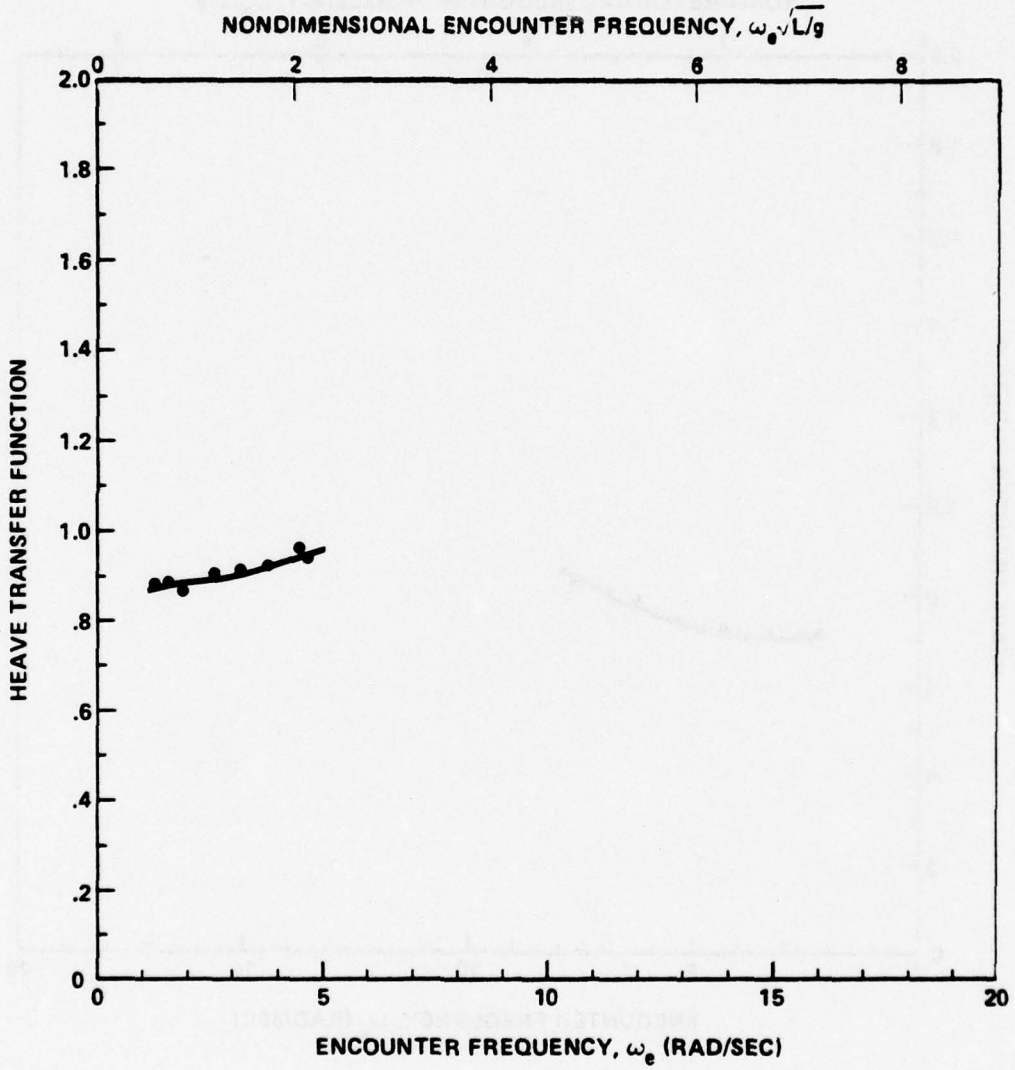


Figure 6a - Heave Transfer Function as a Function of Encounter Frequency for $\lambda/L = 5.17$

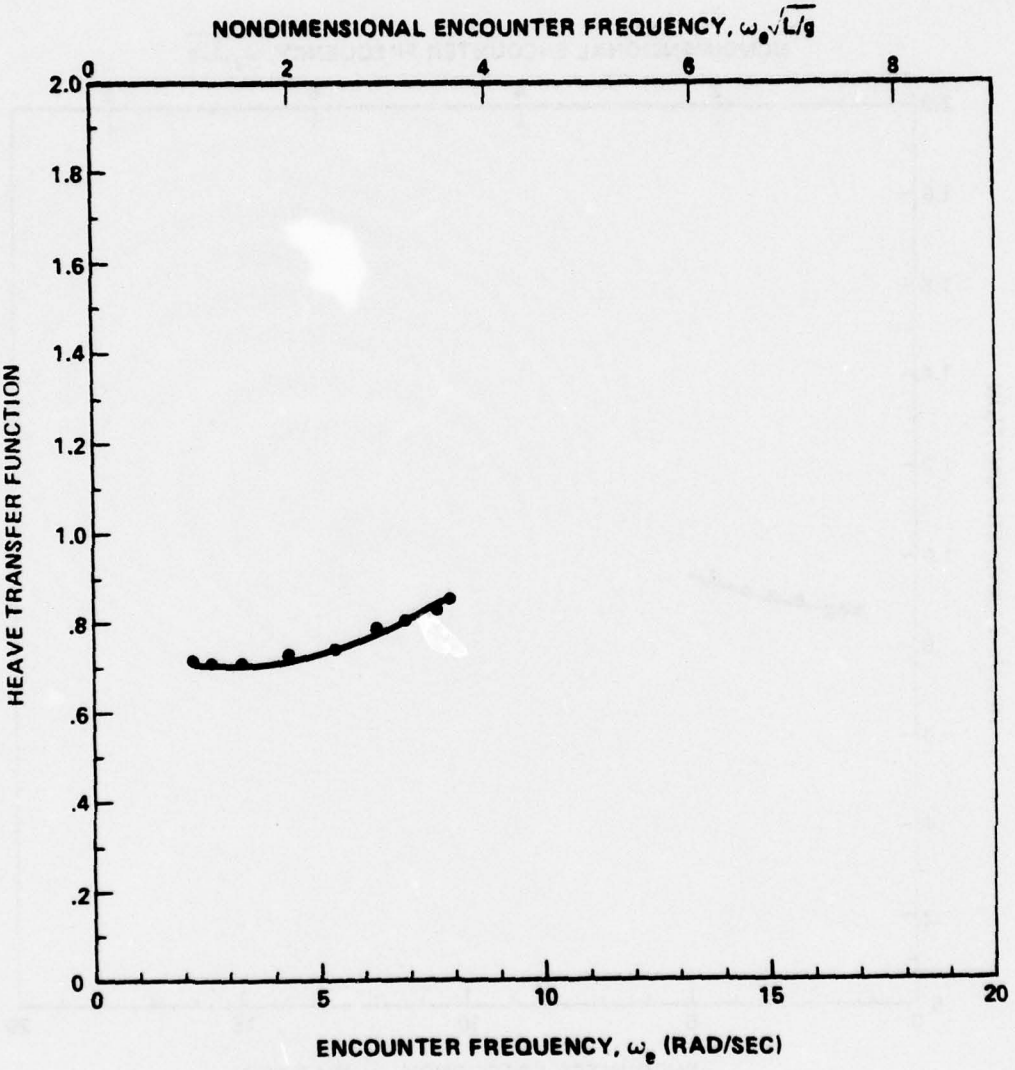


Figure 6b - Heave Transfer Function as a Function of Encounter Frequency for $\lambda/L = 3.04$

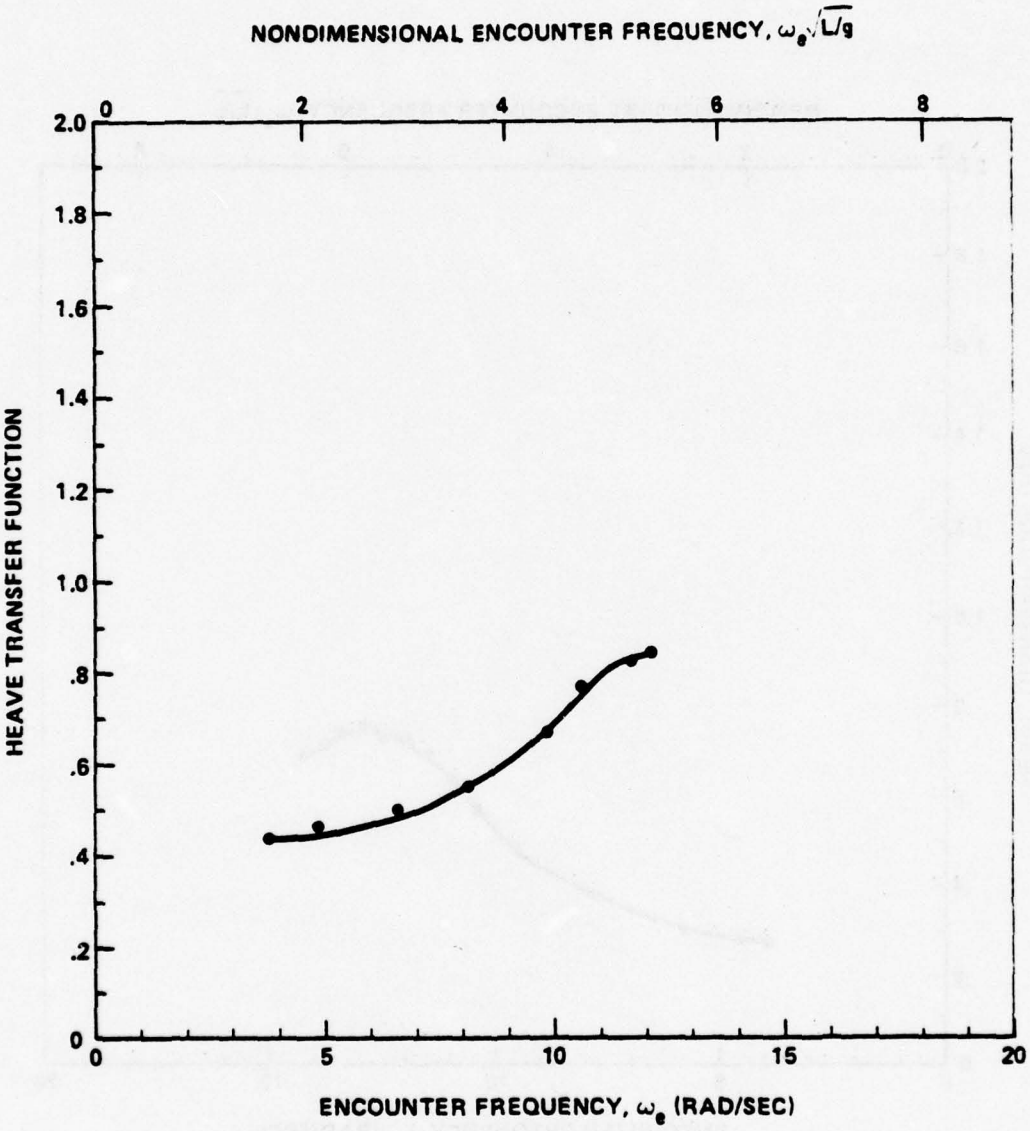


Figure 6c - Heave Transfer Function as a Function of Encounter Frequency for $\lambda/L = 1.98$

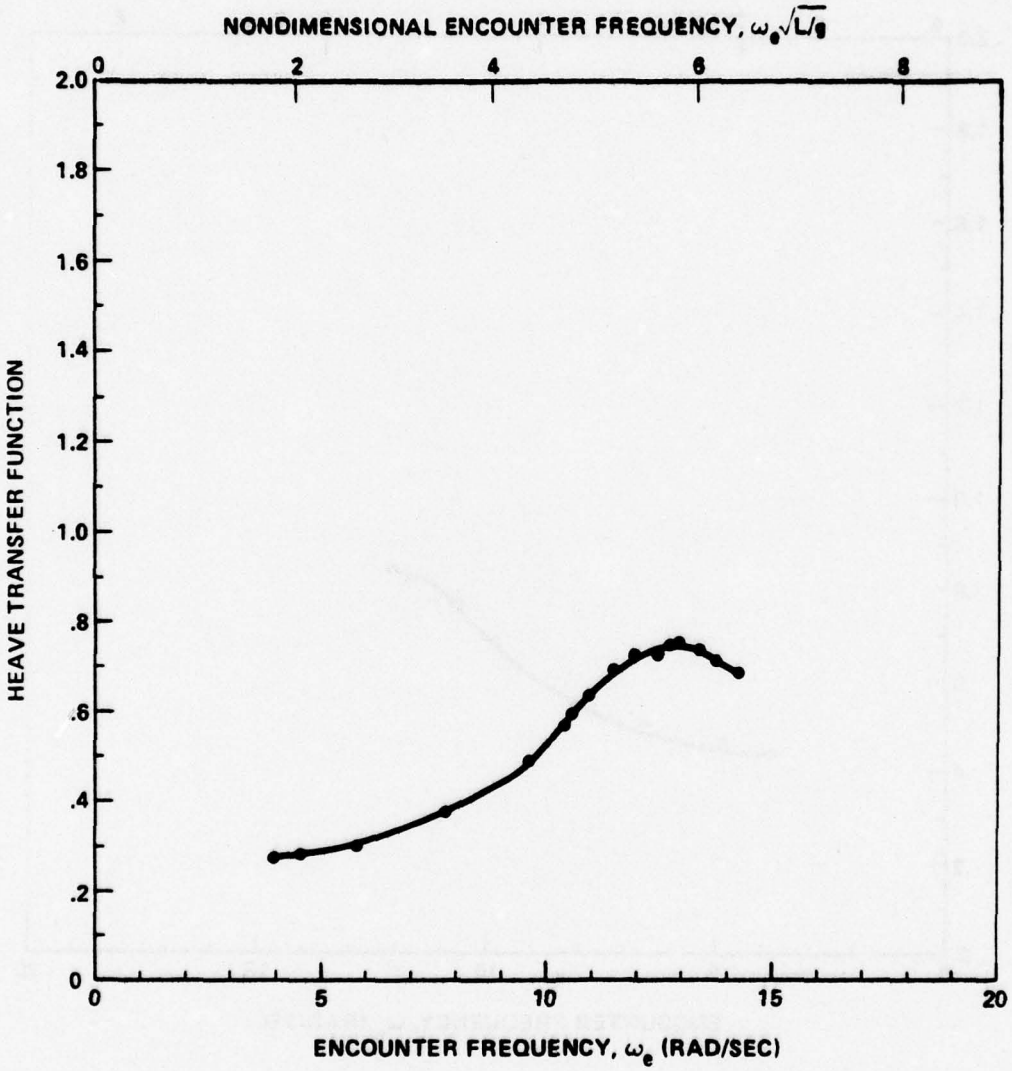


Figure 6d - Heave Transfer Function as a Function of Encounter Frequency for $\lambda/L = 1.67$

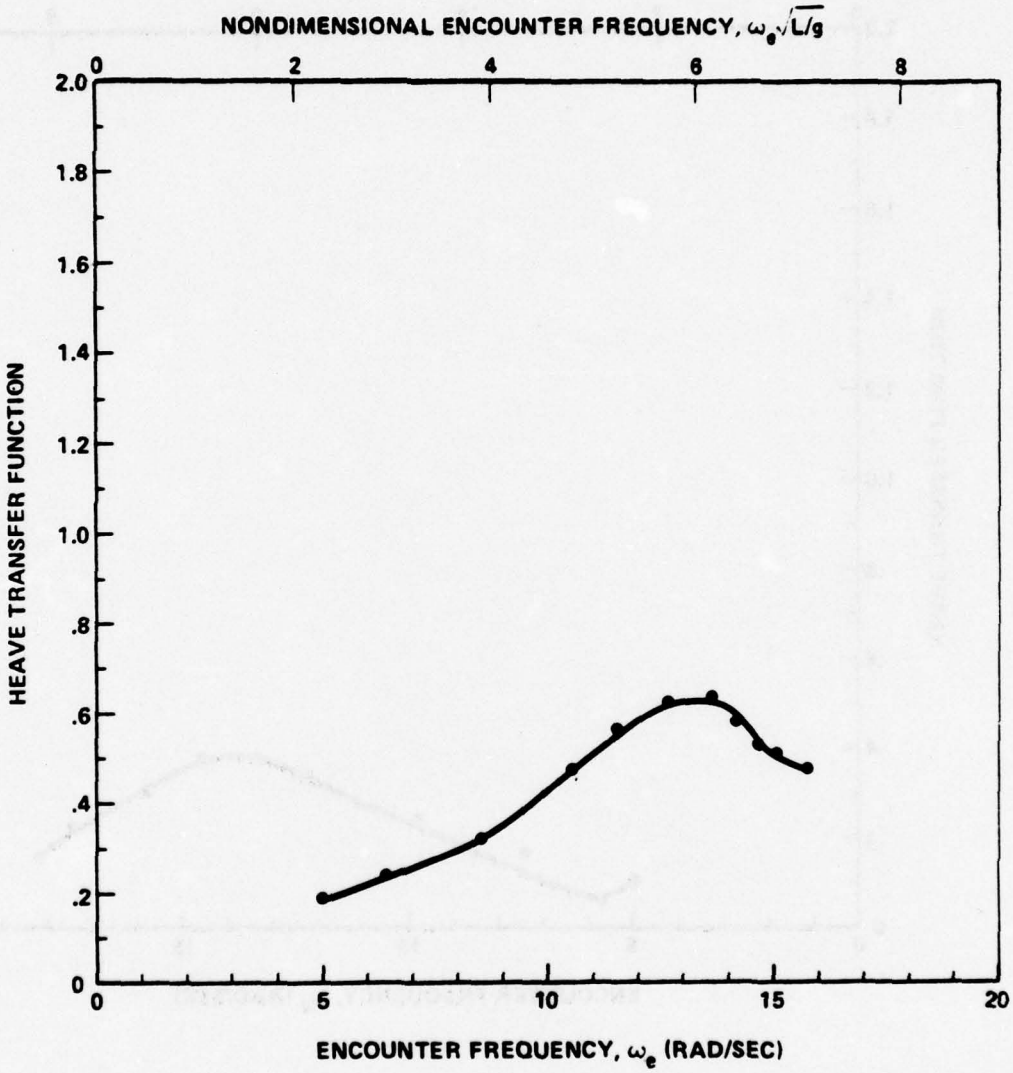


Figure 6e - Heave Transfer Function as a Function of Encounter Frequency for $\lambda/L = 1.52$

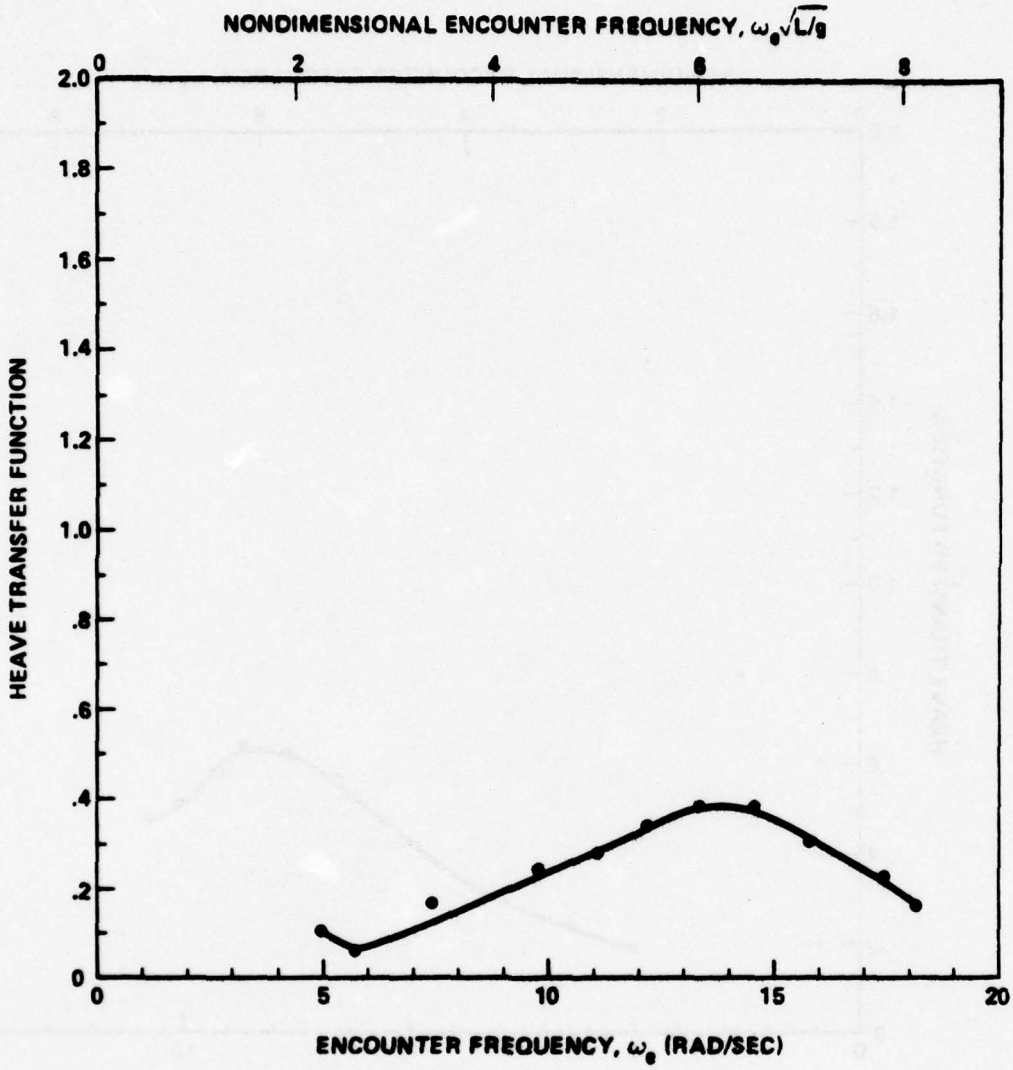


Figure 6f - Heave Transfer Function as a Function of Encounter Frequency for $\lambda/L = 1.32$

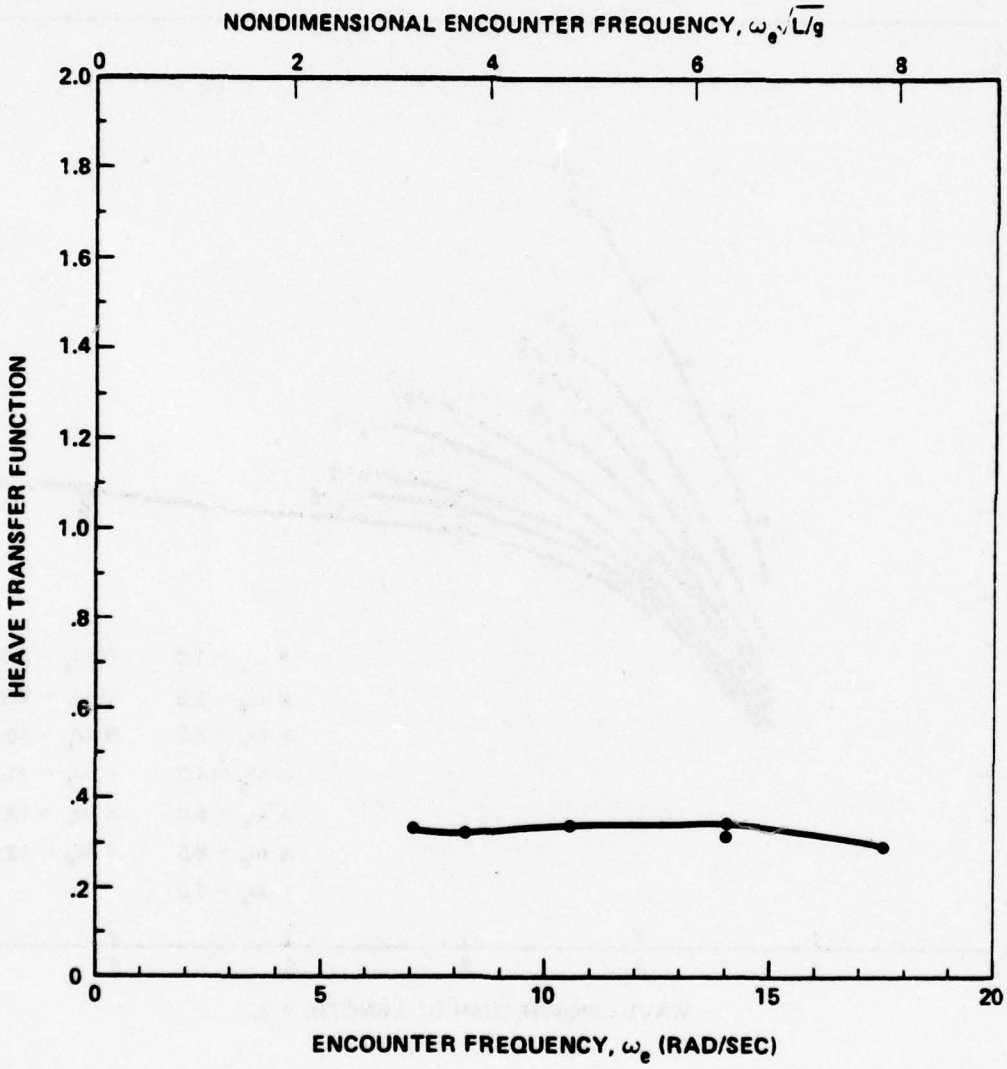


Figure 6g - Heave Transfer Function as a Function of Encounter Frequency for $\lambda/L = .91$

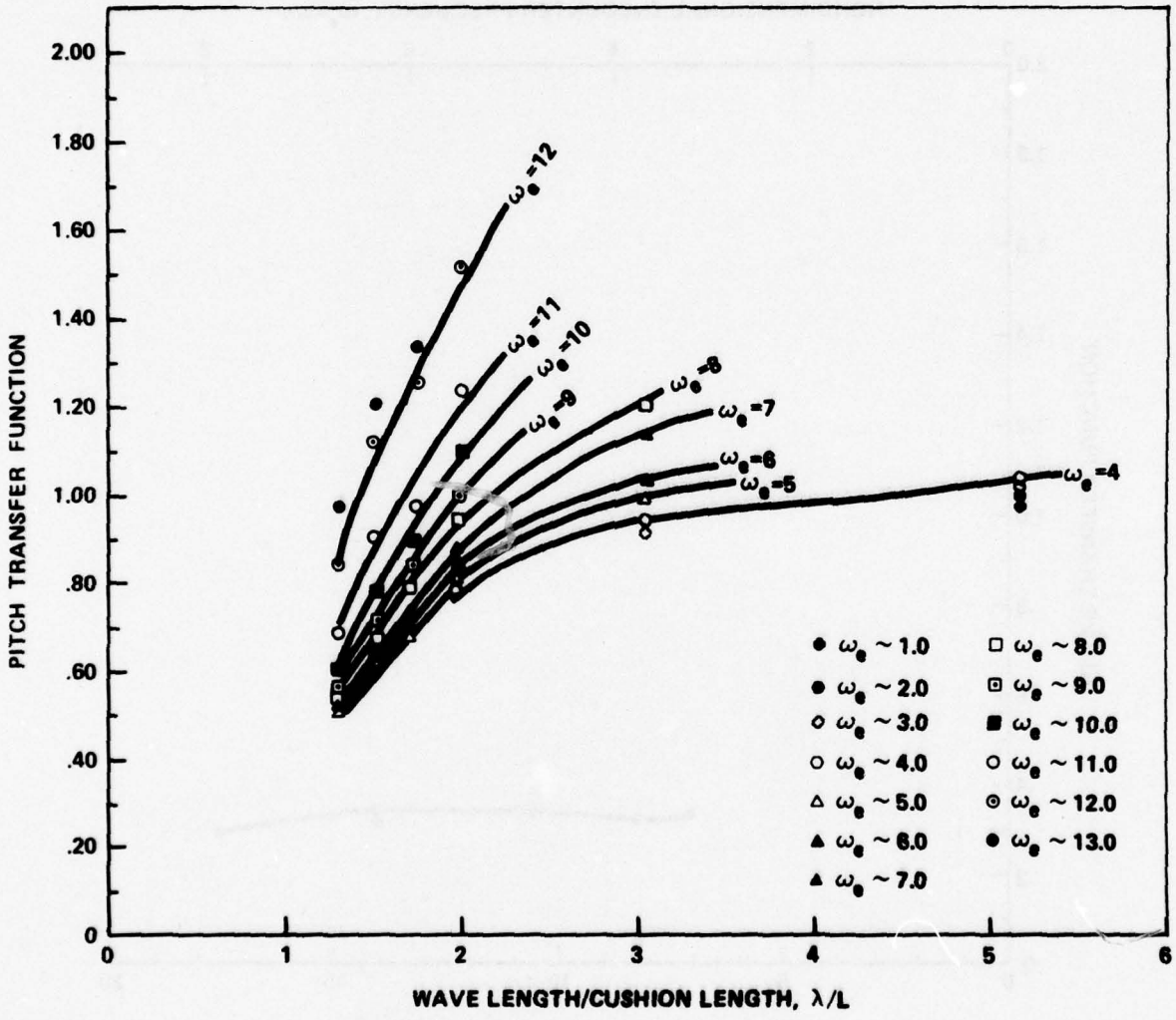


Figure 7 - Pitch Transfer Function as a Function of Wave Length for Constant Encounter Frequency

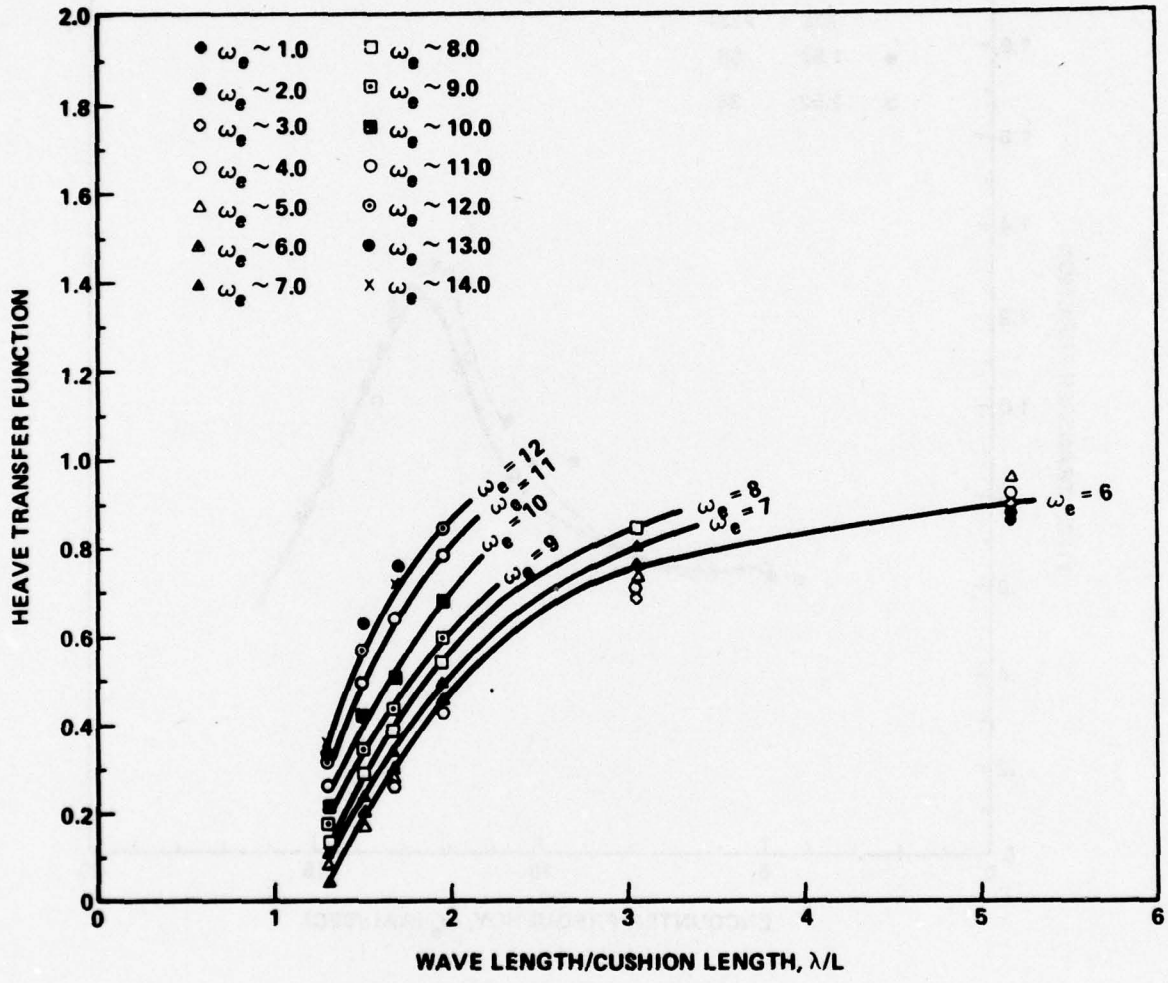


Figure 8 - Heave Transfer Function as a Function of Wave Length for Constant Encounter Frequency

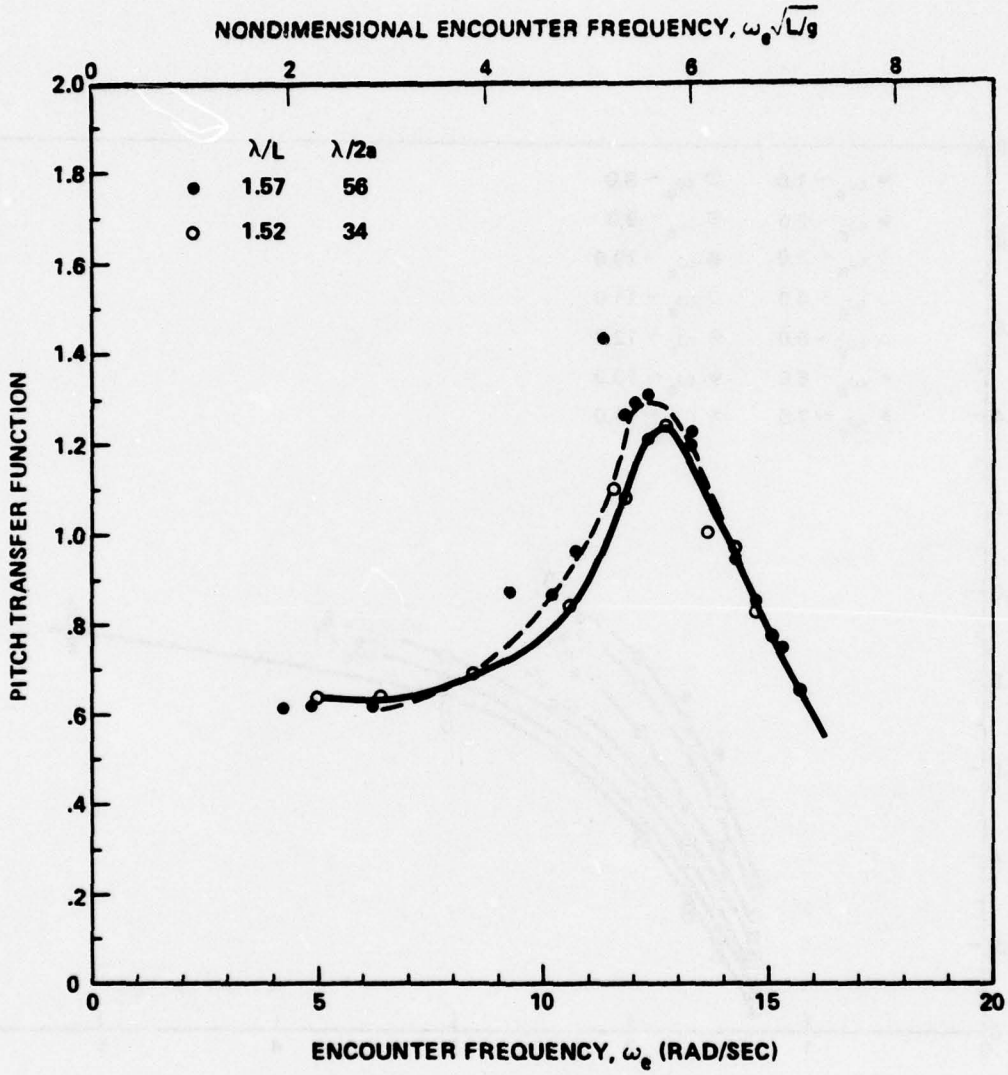


Figure 9 - Pitch Transfer Function as a Function of Encounter Frequency for $\lambda/2a = 34$, 56 and for $\lambda/L = 1.5$

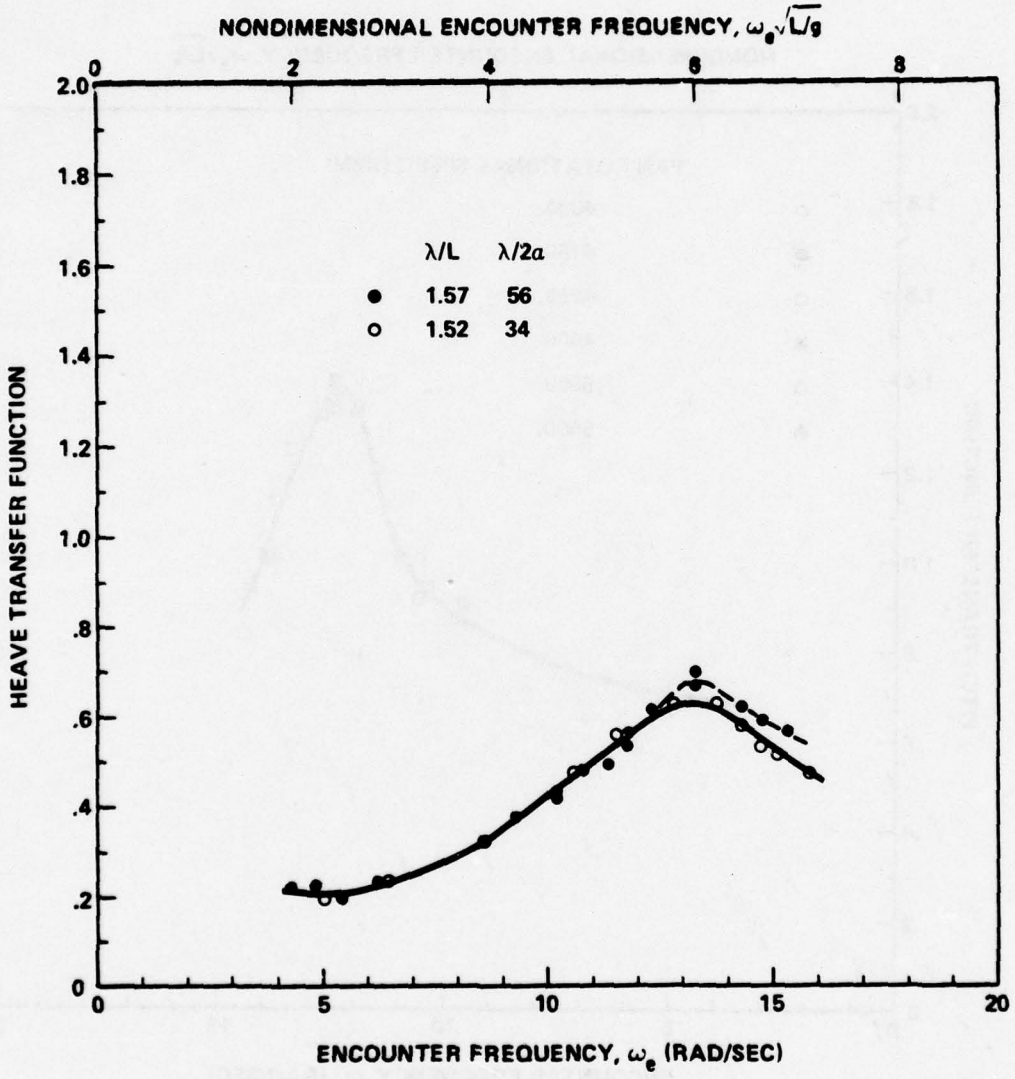


Figure 10 - Heave Transfer Function as a Function of Encounter Frequency for $\lambda/2a$ = 34, 56 and for $\lambda/L$ = 1.5

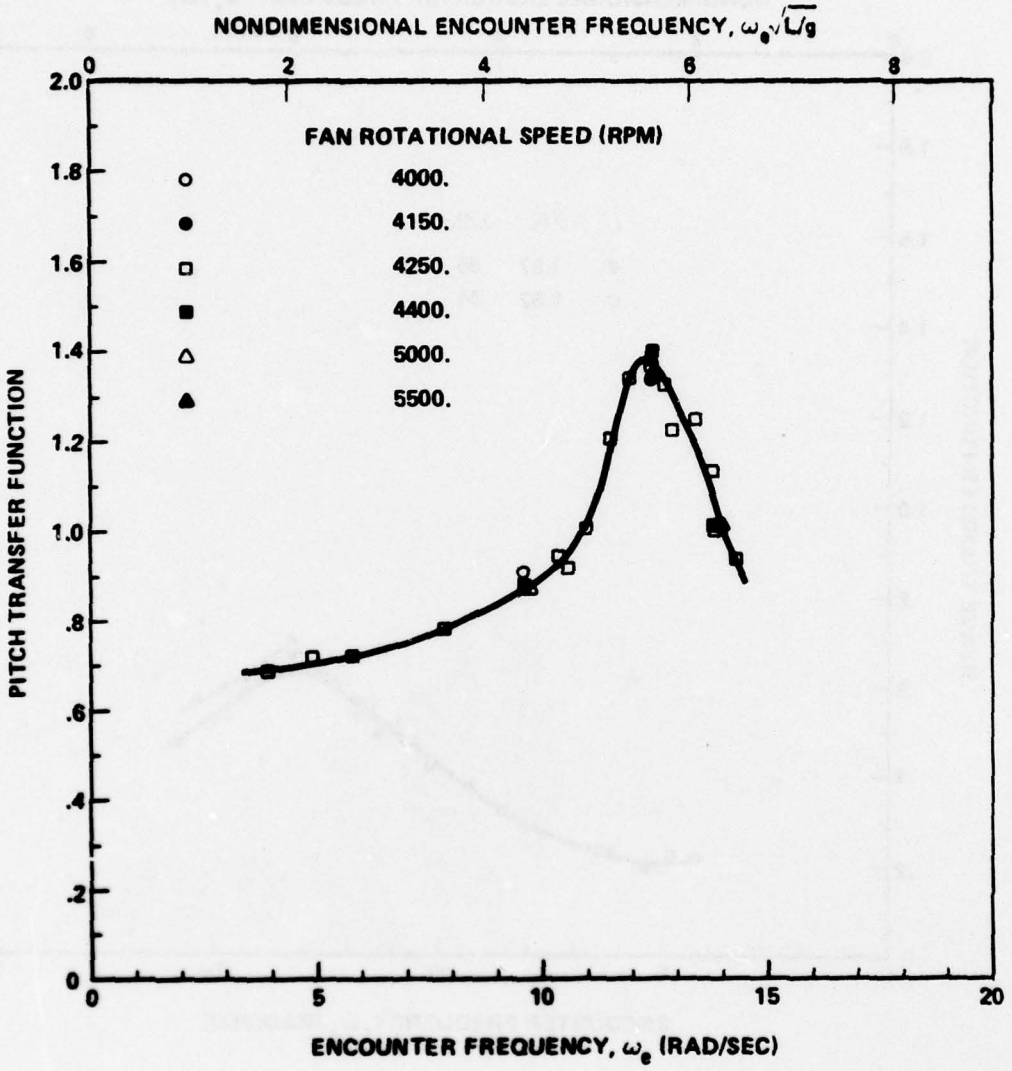


Figure 11 - Pitch Transfer Function as a Function of Encounter Frequency for $\lambda/L = 1.67$ for Various Fan Rotational Speeds

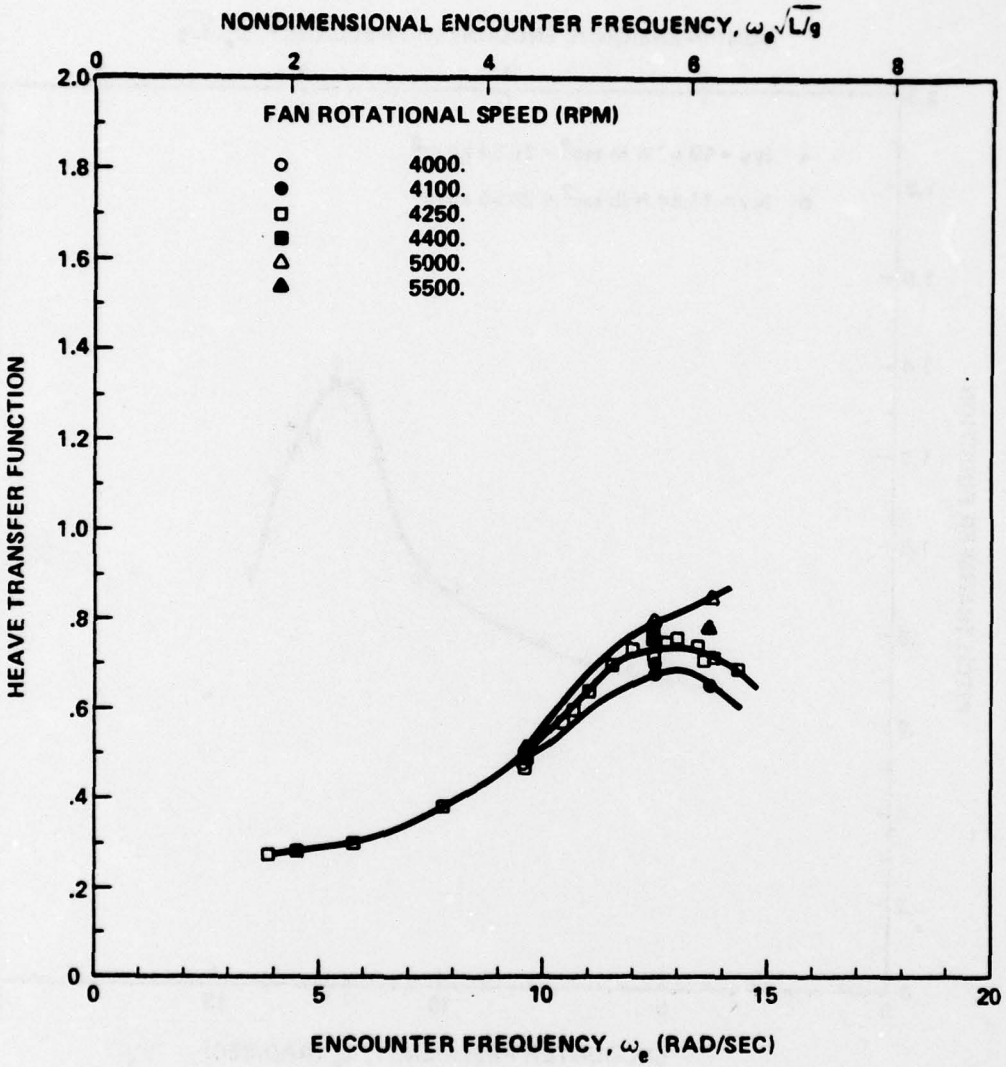


Figure 12 - Heave Transfer Function as a Function of Encounter Frequency for $\lambda/L = 1.67$ for Various Fan Rotational Speeds

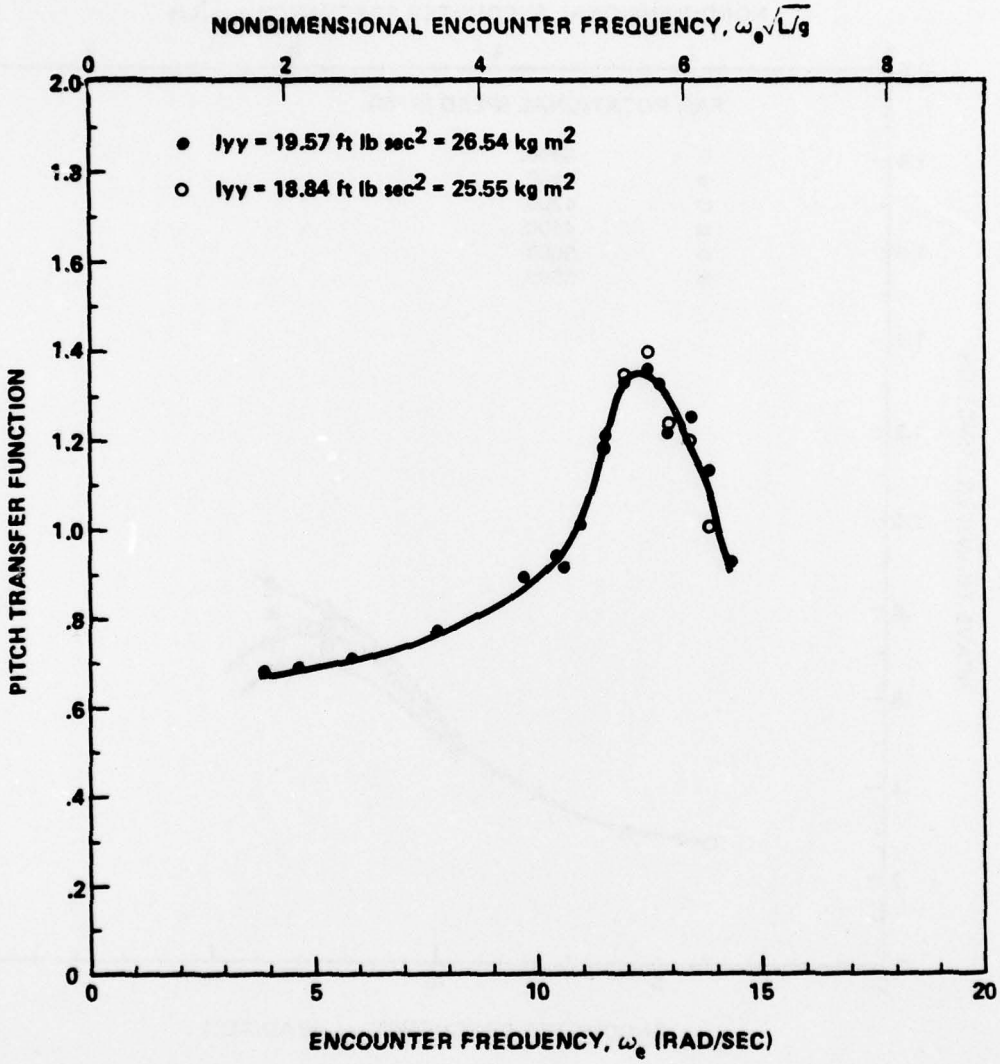


Figure 13 - Pitch Transfer Function as a Function of Encounter Frequency for $\lambda/L = 1.67$ and for Pitch Moment of Inertia Iyy = 19.57 ft lb sec$^2$ (26.54 kg m$^2$) and 18.84 ft lb sec$^2$ (25.55 kg m$^2$)

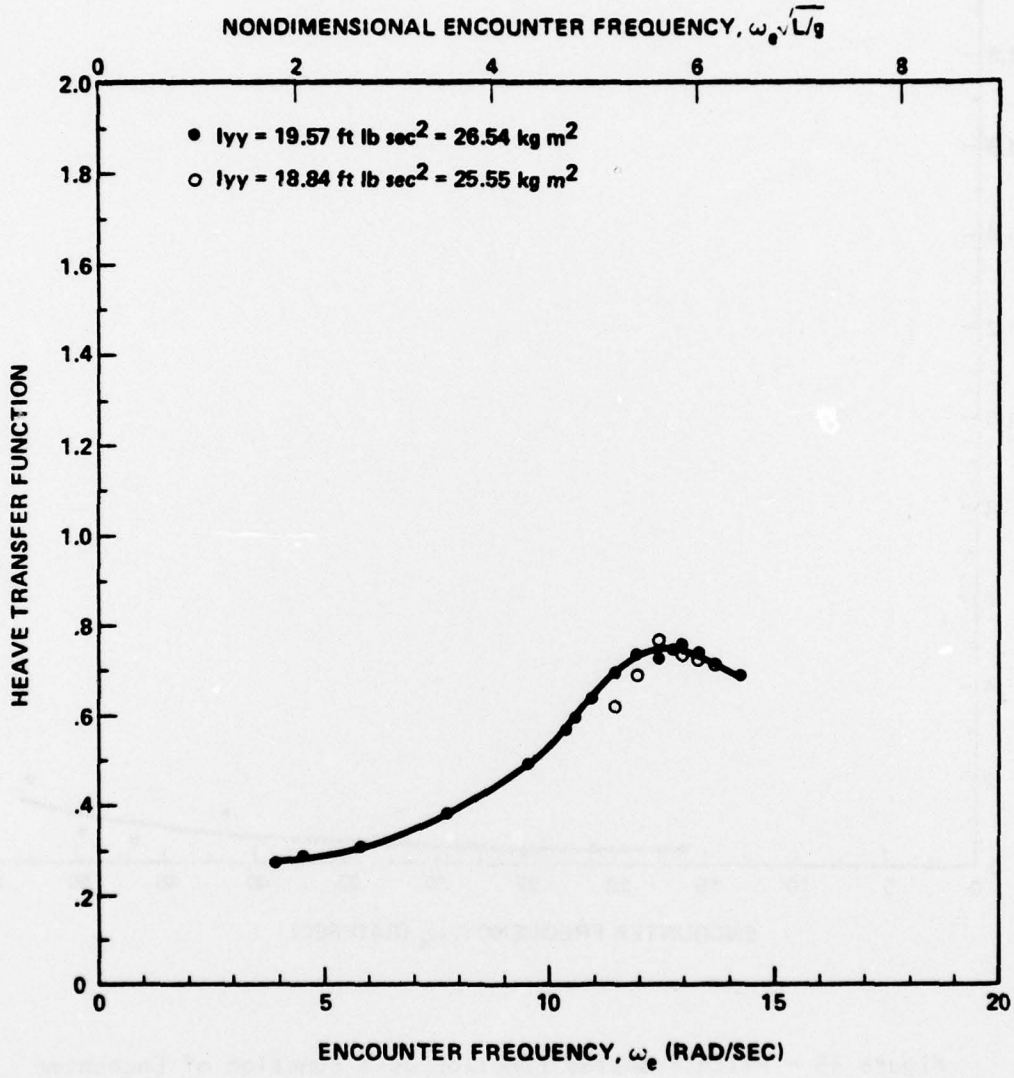


Figure 14 - Heave Transfer Function as a Function of Encounter Frequency for $\lambda/L$ = 1.67 and for Pitch Moment of Inertia Iyy = 19.57 ft lb sec$^2$ (26.54 kg m$^2$) and 18.84 ft lb sec$^2$ (25.55 kg m$^2$)

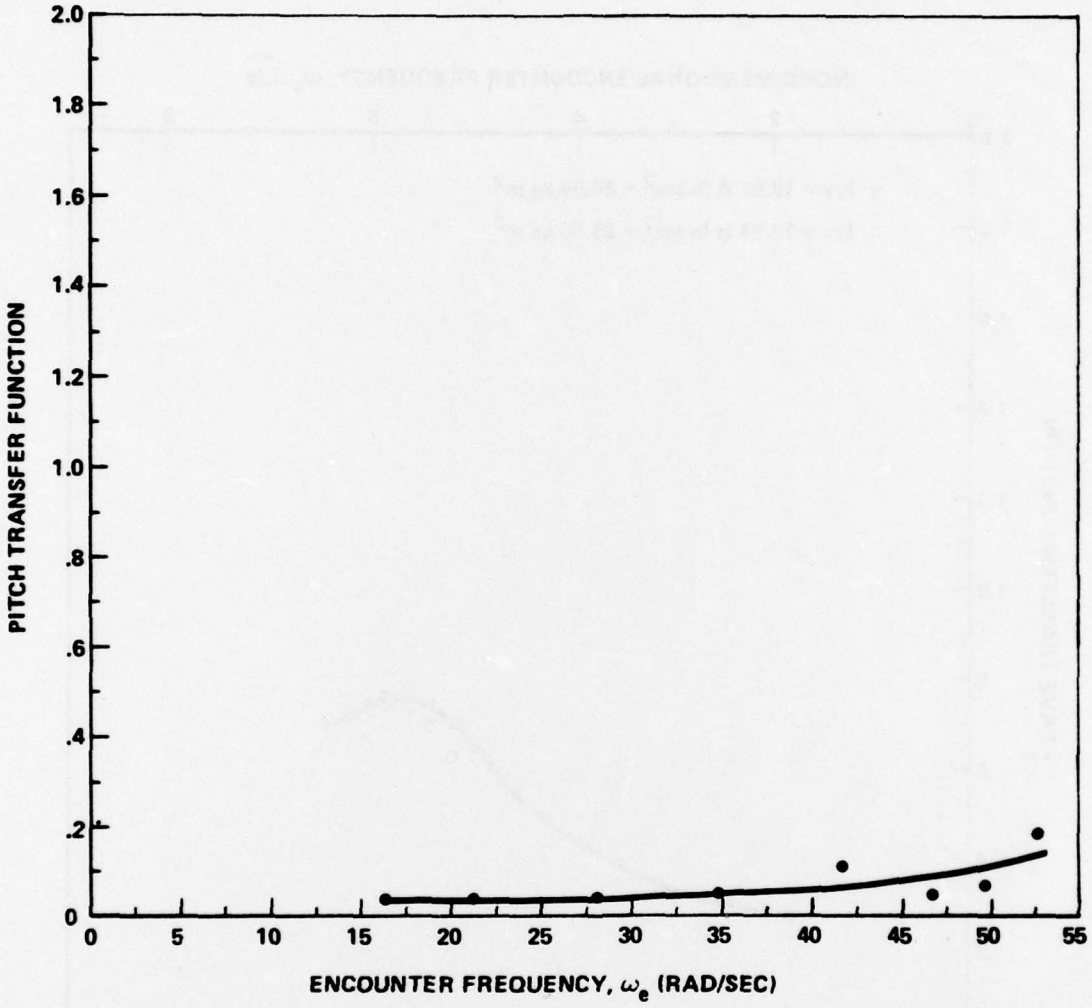


Figure 15 - Pitch Transfer Function as a Function of Encounter Frequency for a Triangular Waveform $\lambda/L = .46$

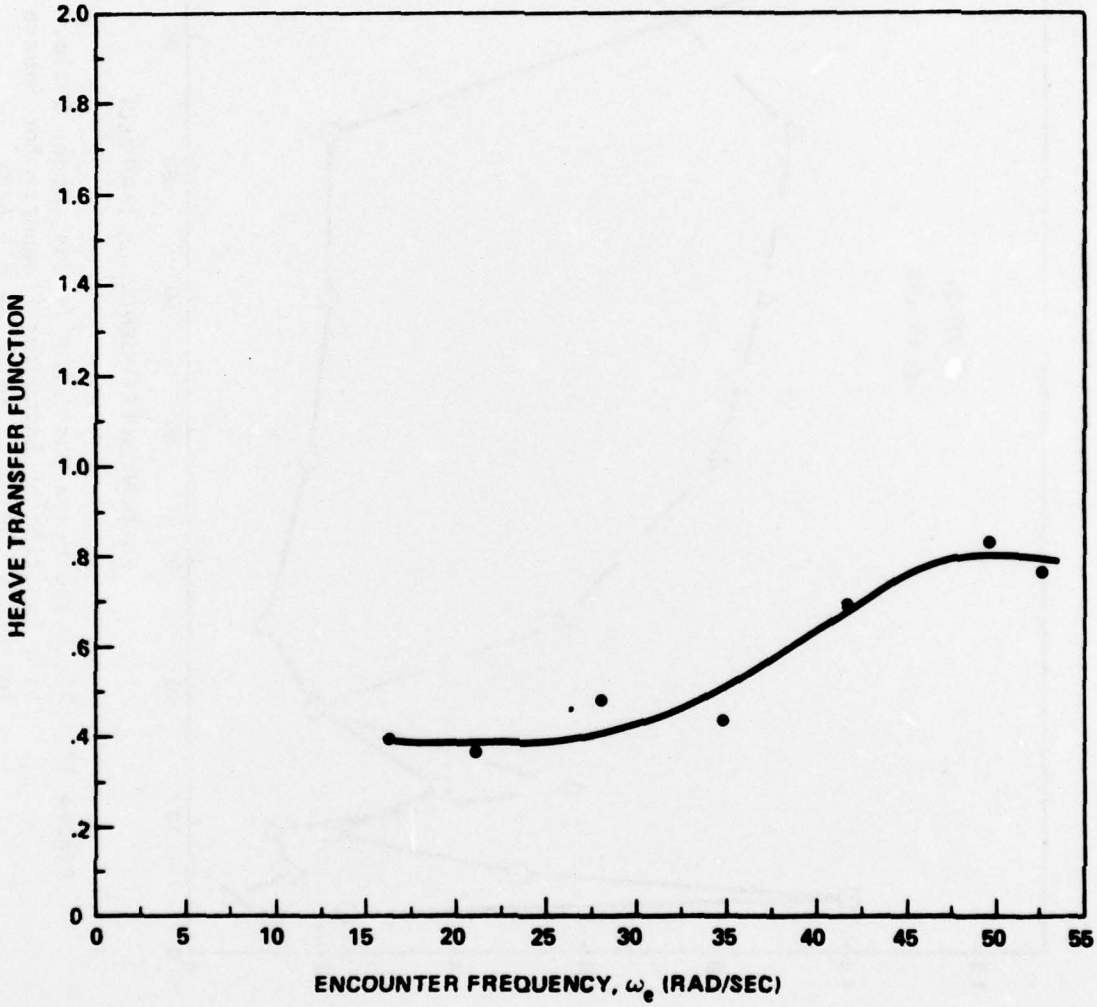


Figure 16 - Heave Transfer Function as a Function of Encounter Frequency for a Triangular Waveform $\lambda/L = .46$

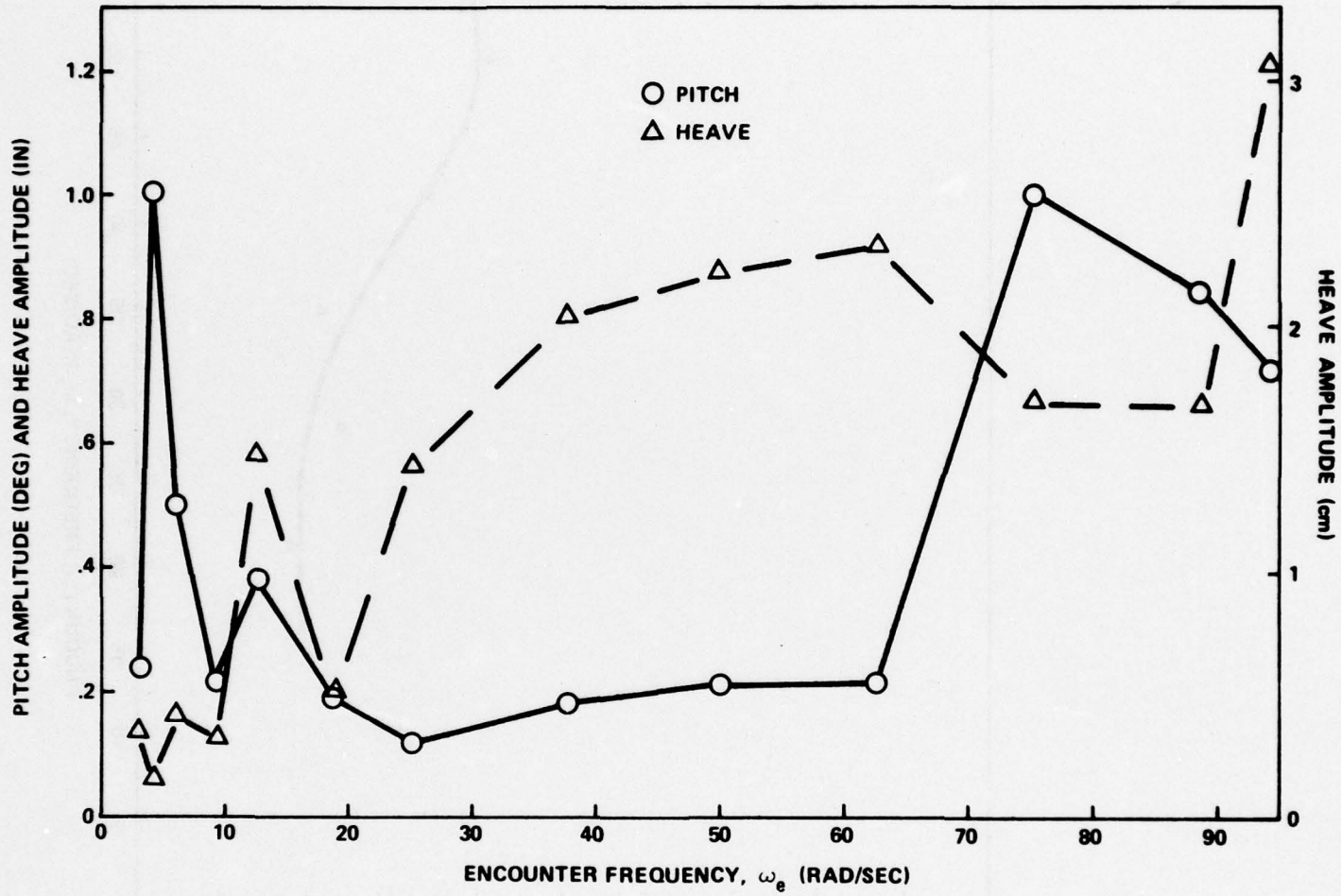


Figure 17 - Pitch and Heave Model Amplitudes, Model Scale, as a Function of Encounter Frequency for Square Wave Excitation for $\lambda/L = .09$, $\lambda = .18$ m, $2a = 4.6$ cm

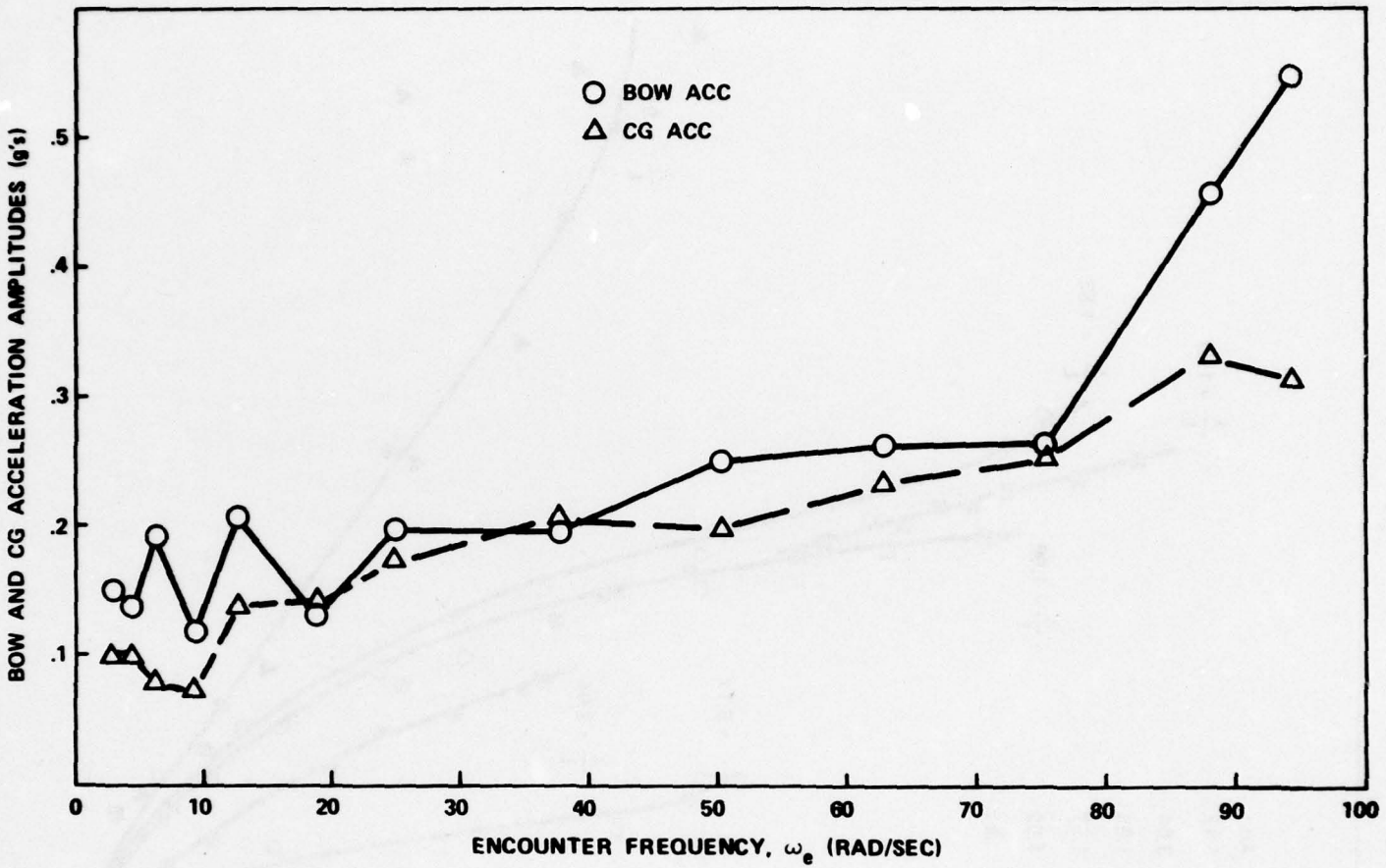


Figure 18 - Bow and CG Acceleration Model Amplitudes, Model Scale, as a Function of Encounter Frequency for Square Wave Excitation for $\lambda/L = .09$, $\lambda = .18$ m, $2a = 4.6$ cm

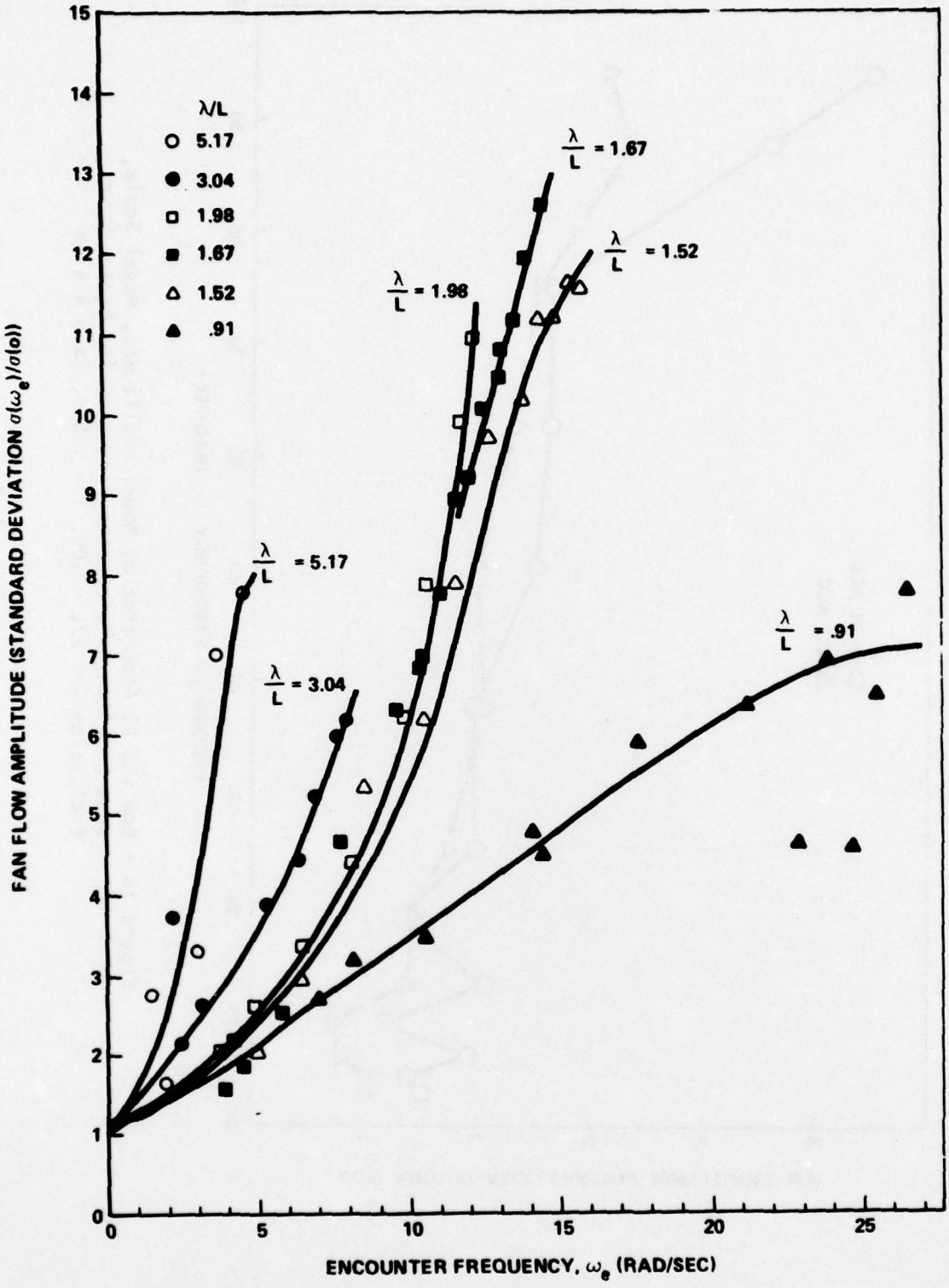


Figure 19 - Fan Flow Amplitude as a Function of Encounter Frequency for Constant Wave Length

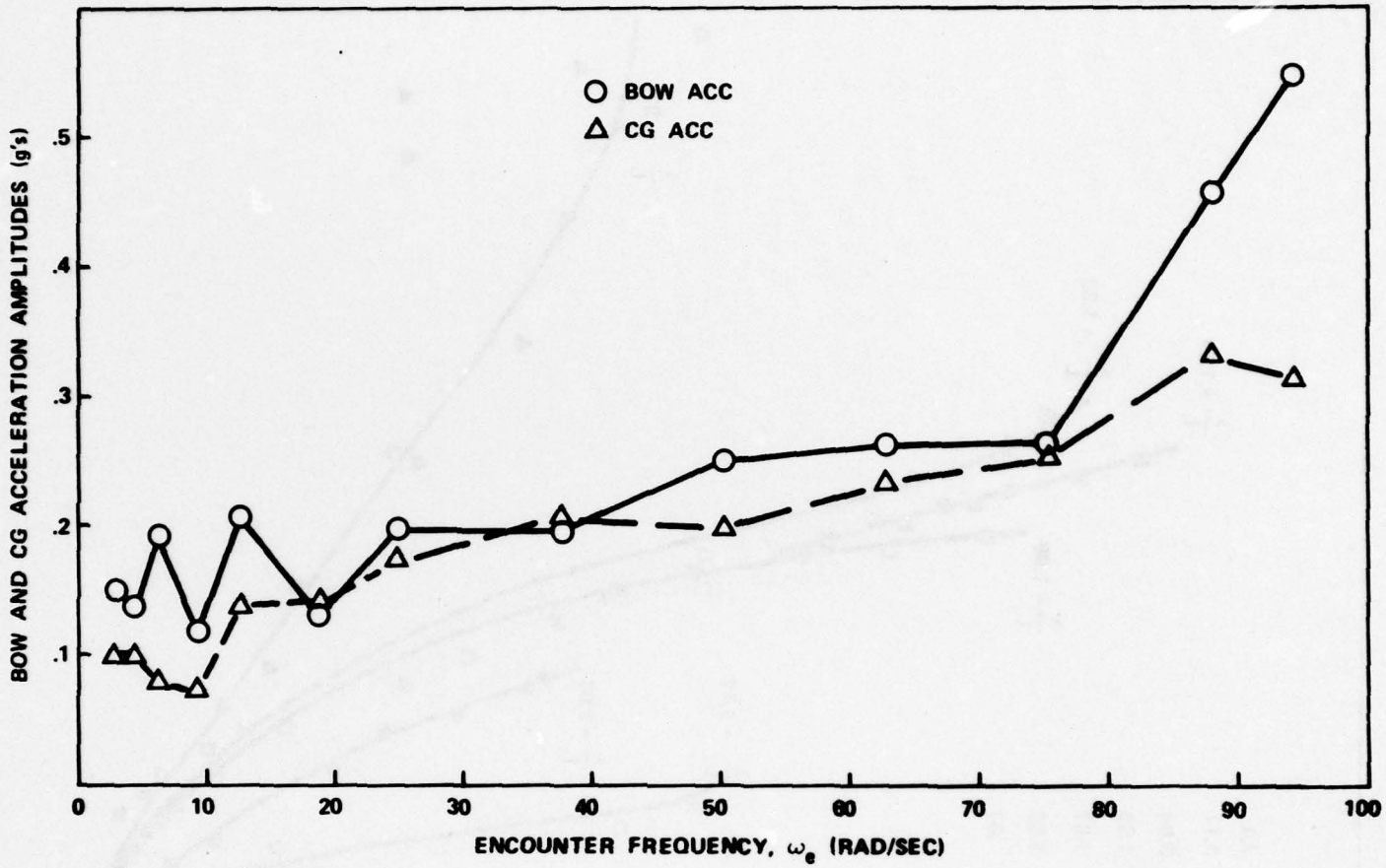


Figure 18 - Bow and CG Acceleration Model Amplitudes, Model Scale, as a Function of Encounter Frequency for Square Wave Excitation for $\lambda/L = .09$, $\lambda = .18$ m, $2a = 4.6$ cm

TABLE I

PHYSICAL CHARACTERISTICS OF THE AALC JEFF (B) MODEL

| | | | |
|---|---|---|---|
| A | Cushion Area | 20.06 $ft^2$ | 6.11 m |
| LOA | Length, overall | 7.30 ft | 222.50 cm |
| L | Length, cushion, effective | 6.58 ft | 200.60 cm |
| BOA | Beam, overall | 3.92 ft | 119.48 cm |
| B | Beam, cushion, maximum | 3.05 | 98.96 cm |
| L/B | Length/Beam Ratio, cushion | 2.16 | |
| M | Mass, tested | 5.41 slugs | 78.9 kg |
| RPM | Fan speed, design, light displacement, rpm | 3750 rpm | |
| $\alpha$ | Angle of bow fingers | $45^o \pm 1^o$ | |
| $h_f$ | Height of bow fingers at noted operating condition | 1.94 < 2.38 in | 4.92 < 6.03 cm |
| | Vertical position of CG with respect to deck, positive upward | .94 in | 2.38 cm |
| | Vertical position of pitch hinge with respect to deck, positive upward | 1.50 in | 3.81 cm |
| | Longitudinal position of CG with respect to stern datum, positive forward | 39.25 in | 99.70 cm |
| | Longitudinal position of pitch hinge with respect to stern datum, positive forward | 39.25 in | 99.70 cm |
| $I_{yy}$ | Pitch moment of inertia | 19.57 ft lb $sec^2$ | 26.53 nt m $sec^2$ |

TABLE 2

OPERATIONAL CONDITIONS

| Wave Form | Wave Length $\lambda$ (ft) | Wave Length $\lambda$ (m) | $\lambda/L$ | Wave Amplitude a (cm) | Wave Slope ka (Degrees) | Ramp Slope (Degrees) | No. of Waves | Model Scale Speed Range (kts) |
|---|---|---|---|---|---|---|---|---|
| Trapezoidal | 34 | 10.4 | 5.17 | 5.3 | 1.9 | 5.2 | 2 | 4-15 |
| Trapezoidal | 20 | 6.1 | 3.04 | 5.1 | 3.1 | 5.2 | 4 | 4-15 |
| Trapezoidal | 13 | 4.0 | 1.98 | 4.8 | 4.4 | 5.2 | 5 | 4.6-15 |
| Trapezoidal | 11 | 3.4 | 1.67 | 4.8 | 5.2 | 5.2 | 5 | 4-15 |
| Trapezoidal | 10.32 | 3.2 | 1.57 | 2.8 | 3.2 | 5.2 | 5 | 4-15 |
| Trapezoidal | 10 | 3.1 | 1.52 | 4.6 | 5.3 | 5.2 | 5 | 4.64-15 |
| Trapezoidal | 8.67 | 2.6 | 1.32 | 4.1 | 5.6 | 5.2 | 5 | 4-15 |
| Trapezoidal | 6 | 1.8 | .91 | 3.0 | 6.1 | 5.2 | 5 | 4-15 |
| Triangular | 3 | .9 | .46 | 1.3 | 5.4 | 5.2 | 5 | 4.64-15 |
| Square | .592 | .18 | .09 | 2.3 | 46 | $\infty$ | 80 | 0.5-15 |
| Level Ground | - | - | - | - | - | 0 | 0 | 4-15 |

TABLE 3

CHARACTERISTICS OF TRAPEZOIDAL WAVEFORMS

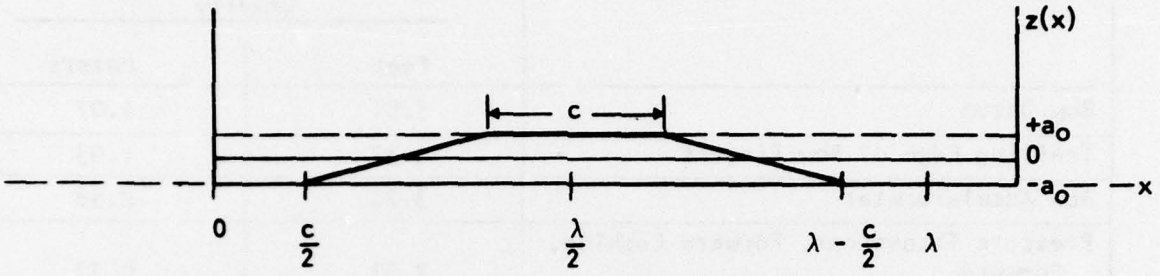


$$z(x) = \frac{-8a_o}{\pi^2 \left(1-2\frac{c}{\lambda}\right)} \sum_{n=1,3,5} \frac{1}{n^2} \cos n\pi \frac{c}{\lambda} \cos \frac{2\pi n x}{\lambda}$$

$$C = \frac{-8a_o}{\pi^2 \left(1-2\frac{c}{\lambda}\right)}$$

| $\lambda/L$ | $c/\lambda$ | $-\frac{C}{a_o}$ | $\frac{1}{n^2}\cos n\pi \frac{c}{\lambda}$ | | |
|---|---|---|---|---|---|
| | | | n=1 | n=3 | n=5 |
| 5.17 | .412 | 4.606 | .273 | -.082 | .0393 |
| 3.04 | ..350 | 2.702 | .454 | -.110 | .0283 |
| 1.98 | .269 | 1.754 | .664 | -.091 | -.0187 |
| 1.67 | .227 | 1.484 | .756 | -.060 | -.0365 |
| 1.57 | .355 | 1.505 | .440 | -.109 | .0304 |
| 1.52 | .200 | 1.351 | .809 | -.034 | -.0400 |
| 1.32 | .154 | 1.171 | .885 | .013 | -.0300 |
| .91 | 0 | .810 | 1.000 | .111 | .0400 |
| .46 | 0 | .436 | 1.000 | .111 | .0400 |

TABLE 4

TRANSDUCER LOCATIONS ON JEFF(B) MODEL

| Transducer of Reference Point | Location Forward of Center of Gravity | |
|---|---|---|
| | Feet | Meters |
| Bow Datum | 3.51 | 1.07 |
| Trailing Edge of Bow Fingers | 3.37 | 1.03 |
| Bow Accelerometer | 3.20 | 0.98 |
| Pressure Transducer, Forward Cushion, Forward | 2.53 | 0.77 |
| Pressure Transducer, Forward Cushion, Aft | 0.87 | 0.26 |
| Trailing Edge, Stability Skirt | 0.16 | 0.05 |
| Pitch-Heave Pivot | 0 | 0 |
| Center of Gravity | 0 | 0 |
| Center of Gravity Accelerometer | 0 | 0 |
| Pressure Transducer, Aft Cushion, Forward | -0.43 | -0.13 |
| Pressure Transducer, Aft Cushion, Aft | -2.40 | -0.73 |
| Trailing Edge of Stern Fingers | -3.21 | -0.98 |
| Stern Datum | -3.27 | -0.99 |

DTNSRDC ISSUES THREE TYPES OF REPORTS

(1) DTNSRDC REPORTS, A FORMAL SERIES PUBLISHING INFORMATION OF PERMANENT TECHNICAL VALUE, DESIGNATED BY A SERIAL REPORT NUMBER.

(2) DEPARTMENTAL REPORTS, A SEMIFORMAL SERIES, RECORDING INFORMATION OF A PRELIMINARY OR TEMPORARY NATURE, OR OF LIMITED INTEREST OR SIGNIFICANCE, CARRYING A DEPARTMENTAL ALPHANUMERIC IDENTIFICATION.

(3) TECHNICAL MEMORANDA, AN INFORMAL SERIES, USUALLY INTERNAL WORKING PAPERS OR DIRECT REPORTS TO SPONSORS, NUMBERED AS TM SERIES REPORTS; NOT FOR GENERAL DISTRIBUTION.